UNIVERSITÀ POLITECNICA DELLE MARCHE

DIPARTIMENTO SCIENZE DELLA VITA E DELL'AMBIENTE

Corso di Laurea Magistrale

Biologia Marina

NEW INSIGHTS INTO THE BIOLOGY OF AGING IN ATLANTIC SWORDFISH (*XIPHIAS GLADIUS*) STOCK

NUOVE RILEVAZIONI SULLA BIOLOGIA DELL'INVECCHIAMENTO NELLO STOCK ATLANTICO DI PESCE SPADA (*XIPHIAS GLADIUS*)

Tesi di Laurea Magistrale di:

Lorenzo Formoso

Relatore:

Prof.ssa Giorgia Gioacchini

Correlatore:

Dott.ssa Giulia Chemello

Sessione straordinaria febbraio 2025

Anno Accademico 2023/2024

RIASSUNTO

Lo stato degli stock di *Xiphias gladius* nell'Atlantico e nel Mediterraneo è preoccupante a causa del sovrasfruttamento. Per ottimizzare la gestione delle risorse, è cruciale integrare i dati sull'età nelle valutazioni degli stock. Questo studio ha l'obiettivo di valutare i cambiamenti epigenetici legati all'età del pesce spada. A questo scopo, sono state utilizzate tecniche avanzate di sequenziamento, analisi bioinformatiche e di machine learning per la valutazione della correlazione tra i livelli di metilazione dei siti CpG e la lunghezza dell'animale e quindi dell'invecchiamento. Le analisi di Gene Ontology (GO) e KEGG Pathway enrichment, condotte su geni in cui ricadono i 19051 CpGs correlati alla lunghezza, hanno messo in evidenza i processi biologici e i pathway molecolari che vengono modulati con l'invecchiamento. È stato inoltre sviluppato un "orologio epigenetico" basato su 57 siti CpG, che rappresenta uno strumento che offre nuove prospettive per la gestione sostenibile degli stock di pesce spada e potrebbe avere implicazioni per altre risorse ittiche a livello globale.

ABSTRACT

The status of *Xiphias gladius* stocks in the Atlantic and Mediterranean is concerning due to overexploitation. To optimize resource management, it is crucial to integrate age data into stock assessments. This study aims to evaluate the epigenetic changes associated with the age of swordfish. To achieve this, advanced sequencing techniques, bioinformatics analysis, and machine learning were used to assess the correlation between CpG site methylation levels and the animal's length, and thus its aging process. Gene Ontology (GO) and KEGG Pathway enrichment analyses, conducted on genes associated with the 19,051 CpGs related to length, highlighted the biological processes and molecular pathways modulated by aging. Additionally, an "epigenetic clock" based on 57 CpG sites was developed, providing a tool that offers new perspectives for the sustainable management of swordfish stocks and could have implications for other global fishery resources.

INDEX

1. INTRODUCTION

1.1 *Taxonomy of billfish*

In the Perciformes order, the term “billfish” is used to identify individuals in the Xiphioidei suborder belonging to the families of Istiophoridae and Xiphiidae. The Istiophoridae family consists of five genera: *Istiophorus* (Sailfish), *Istiompax* (Black marlin), *Makaira* (Blue marlin), *Tetrapturus* (Spearfishes) and *Kajikia* (Striped marlin), which are represented by a total of nine species. While the Xiphidae family is composed of one genus and one species: *Xiphias gladius* (Linnaeus, 1758) (Collette et al., 2006). Members of the family Xiphiidae are morphologically different from those of the Istiophoridae based on the number of keels on each side of the caudal peduncle, the shape of the bill, the length of the dorsal fin base, the number of vertebrae, the absence of pelvic fins, lateral line, jaw teeth and scales in adult fishes (Collette et al., 2006).

To place an organism in its respective taxon, other than morphological characteristics also specific measurements are used to identify different billfish species (Figure 1) (Collette et. al., 2006; Integrated Taxonomic Information System (ITIS); Mamoozadeh et al., 2023).

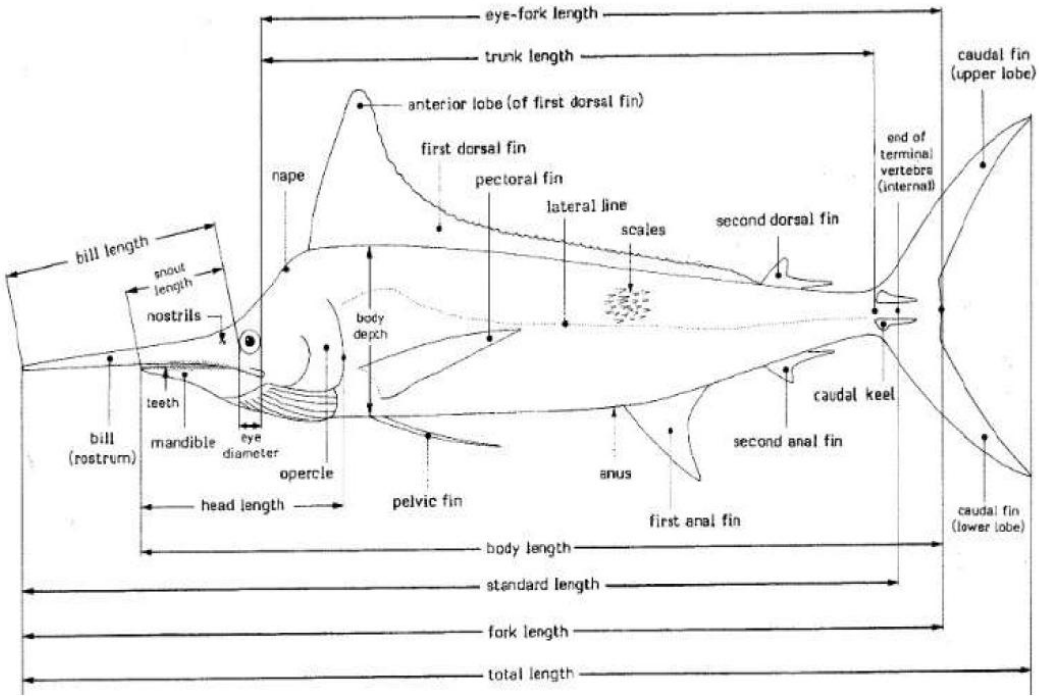

Figure 1*: distinctive traits and biometrics for billfish taxonomy (Surya et al., 2022).*

1.2 *The biology of Xiphias gladius*

Commonly known as "swordfish" (Figure 2), *Xiphias gladius* is the only member of the Xiphidae family. It can be recognized by its elongate cylindrical body with two dorsal fins well separated in adults with the first much larger than the second one, low pectoral fin insertion, absence of pelvic fins, a single median keel on both sides, two separate anal fins in adults with the first larger than the second. It also presents an extremely flattened long bill, not protrusible mouth, exceptionally large eyes, and a single large swim bladder. Scales, jaw teeth and lateral line, are absent in adults, while they are present in young

individuals of about 1 meter (Nakamura, 1985; FAO, 2024). The body color is blackish-brown, and it gradually fades to light brown on the ventral side. Females grow faster than males and reach a larger maximum size. The biggest swordfish ever recorded is an individual of unknow sex of 536,15 Kg caught off the coast of Iquique (Chile) in 1953 (Nakamura, 1985; Surya et al., 2022; ICCAT, 2023; FAO, 2024).

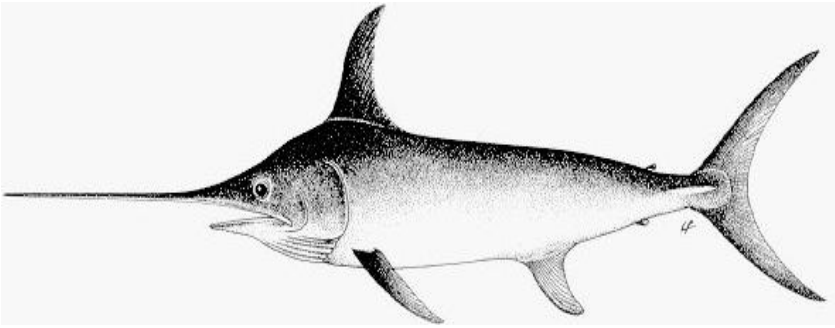

Figure 2: *the "swordfish", Xiphias gladius (FAO, 2024).*

The swordfish presents other different peculiarities that distinguish it from all other Perciformes, such as an oil-producing gland positioned at the base of the rostrum just in front of the eyes (Figure 3) (Videler et al., 2016). This area is rough, porous and little mineralized, it is connected to a system of small vessels that carry the oil to pores around the whole head of the swordfish. Water pressure allows the oil to be released on the surface of the head, thus creating a hydrophobic layer that reduces friction during movement (Lerner et al., 2013; Habegger et al., 2015; Videler et al., 2016).

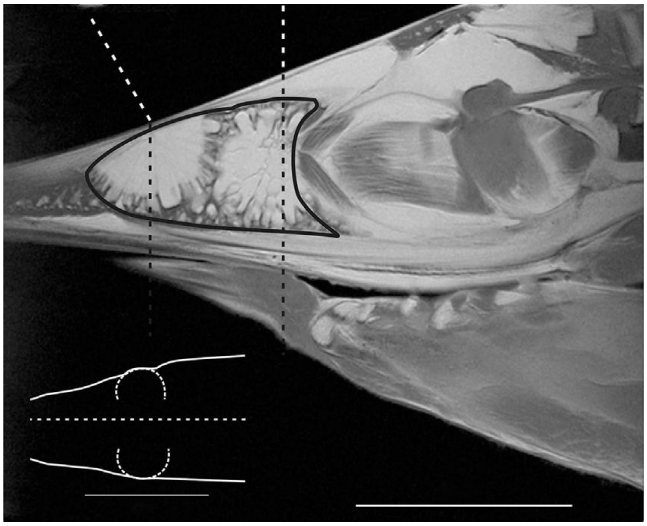

Figure 3: *sagittal MRI section of swordfish head, the oil gland is outlined in black. The three parts of the gland are highlighted by the dashed lines (Videler et al., 2016).*

Another singularity of the swordfish is the ability to exclusively warm up the central nervous system including its big eyes, this characteristic facilitates life at low light intensities and low temperatures (Fritsches et al., 2005). A highly specialized heating system is located in the extraocular muscle, it can heat up to 10-15°C above water temperatures. This capacity increases visual resolution and consequently prey detection when hunting in deep and cold waters (Fritsches et al., 2005).

As an ectothermic species, the swordfish regulates its internal temperature based on the temperature of the marine environment. A rudimentary thermoregulation system allows the swordfish to control its body heat exchange, making it capable of dealing with a wide range of different seasonal or daily changes in environmental parameters (Stoehr et al., 2018).

To explain the biological mechanism behind this regulation, it is necessary to specify that the swordfish is characterized by two types of muscle fibers, the white muscle and the red muscle fiber, the latter is solely used by the animal to swim and the other is used during short-duration burst swimming. These muscle fibers are supplied by two blood circulatory systems: a central and a peripheral one. When swordfish descend to a greater depth, the environmental temperature decreases, so the rate of heat exchange is slowed down from 8 to 13 times. This is possible through the vase restriction of the peripheral circulatory system allowing heat conservation in the central circulatory system (Stoehr et al., 2018). This mechanism allows the red muscle fibers (RM) to stay warm for about 8 hours. During this time the stored heat dissipates slowly until the swordfish need to reach shallow warmer water to recover the heat loss. To do so, the swordfish ascends from the depth, the environmental temperature increases, and the peripheral circulatory system undergoes vasodilation channeling the blood from the central circulatory system (Stoehr et al., 2018).

Last but not least, *X. gladius* is a continuous swimmer, and it breathes using ram ventilation, which means that the fish can breathe passively while swimming with the mouth open through which the water flows to the gill chamber, where it is slowed down to allow gas exchange (Wegner et al., 2012). The swordfish has developed a peculiar fusion of the branchial filaments that

make the gill chamber more resistant to the high pressure of water by reinforcing the respiratory surfaces and keeping it stable to the income flow, maintaining functional ram ventilation despite the high speed reached by this species (Wegner et al., 2013).

1.3 *Distribution, migrations and feeding behaviour*

X. gladius is an epi-mesopelagic species, it has a wide geographical distribution in all the oceans and the Mediterranean Sea. Its optimal habitat is between 45°S and 45°N including all tropical, subtropical, and temperate seas, except in the North Atlantic where it extends farther north, up to 60°N (Figure 4) (Erauskin-Extramiana et al., 2020). For this reason, it is more common to find high densities of swordfish in the Atlantic Ocean, nonetheless, high abundances were also found in the Southeast Pacific and tropical areas close to the Greenwich meridian (Palko et al., 1981; Erauskin-Extramiana et al., 2020).

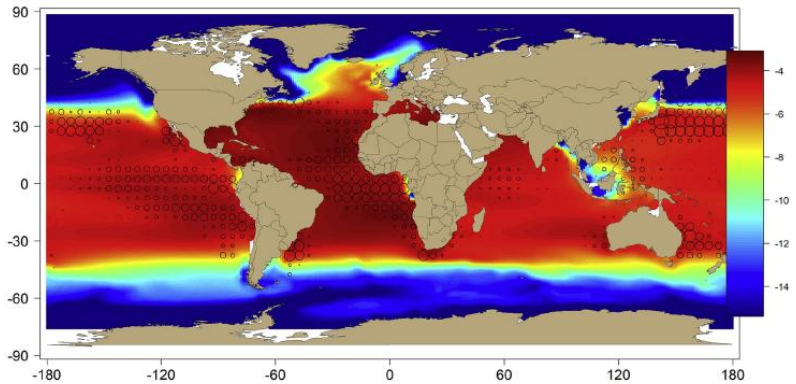

Figure 4: *swordfish habitat distribution model. Red zones represent the optimum habitat and most populated areas of the swordfish. White areas represent a lack of data. Black circles represent the Catch Per Unit Effort (CPUE). The size of the circles is proportional to the CPUE (Erauskin-Extramiana et al., 2020).*

The swordfish migration patterns reveal its feeding behavior. It was observed that in spring and summer, the swordfish performs seasonal horizontal feeding migrations moving northwards, while in autumn and winter, it moves southwards (Nakamura, 1985; Abascal et al., 2010; FAO, 2024). It always follows currents that are cold and rich in food, for example, the Gulf Stream (rich in food) and the North Atlantic cold waters encounter creates an important swordfish's feeding ground and it plays an important role also in its reproduction patterns (Abascal et al., 2010; Abascal et al., 2015).

Indeed, swordfish migration patterns are also based on the location of breeding events. The main spawning areas are the Atlantic Ocean (Caribbean, Gulf of Mexico, and Florida), the Central and the Southwestern Pacific Ocean, the Mediterranean Sea and all around the world at the Equator (Nakamura, 1985; FAO, 2024). In the Mediterranean Sea, the spawning areas are located in the southern regions of Italy, especially in the Strait of Messina (Nakamura, 1985; FAO, 2024).

In addition to horizontal migrations, acoustic telemetry and archival tagging have also documented vertical movement patterns showing a model of daily vertical migration. Generally, specimens make vertical movements from the warm surface layer (18-24°C) to cold waters (8°C) below the thermocline, however, its presence was recorded in waters as deep as 1664 mt (Braun et al.,

2019) reaching water temperatures as low as 2ºC (Takahashi et al., 2003). Most of the day is spent at great depths, only at night they prefer to return to shallow waters. Individuals have also shown the so-called "basking events," defined as a "rapid ascent from depth to spend at the surface a period ranging from minutes to hours, then followed by a rapid descent" (Figure 5) (Stoehr et al., 2018; Rosa et al., 2022).

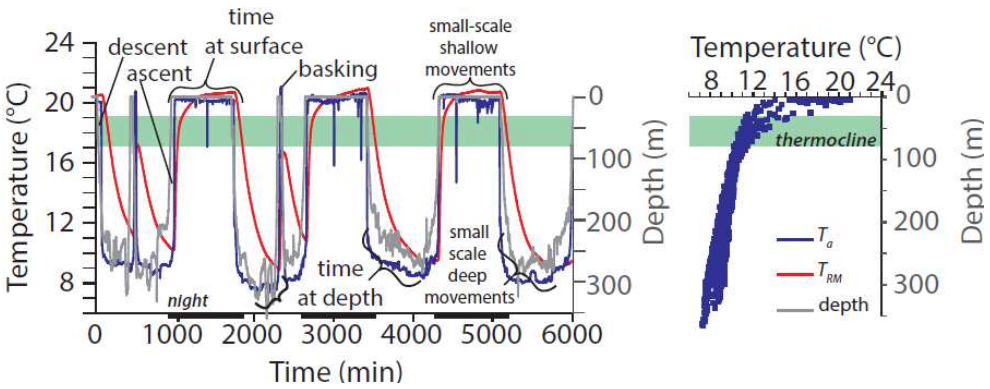

Figure 5: *vertical movement patterns of free-swimming swordfish (left panel) and water temperature-depth profiles (right panel). T_{RM} is the red muscle temperature; T_a is the ambient temperature (Stoehr et al., 2018).*

Despite these movements require a considerable amount of energy spent in thermoregulation and in adaptation to environmental changes, it contributes to the ability of swordfish to hunt at great depth avoiding competition with other pelagic predators. However, swordfish recover their physical energy, by staying in more shallow waters during the night (Stoeher et al., 2018).

The daily vertical migrations are mainly linked to the feeding habits of this species, the swordfish is a generalist and opportunistic apical predator of the

marine food webs, hunting over a wide range of species distributed along a great depth range (Stoeher et al., 2018). It has been highlighted the possibility that *X. gladius* uses its sword to occasionally kill its preys, analyses of stomach contents show clear marks of slashes caused by the sword on preys' body (Logan et al., 2021). Reports on the feeding habits of the swordfish highlighted that the diet of this species always includes squids (*Ommastrephes* gen., *Loligo* gen., *Illex* gen.) and teleosts, and it changes consistently at the regional level (Nakamura, 1985; FAO, 2024 and Logan et al., 2021). The diet of swordfish in depth habitats includes, among others: tuna (*Thunnus* gen.), dolphinfish (*Coryphaena* gen.), flyingfish (*Exocoetidae* gen.) and barracuda (*Sphyraenidae* gen.). Only large adults often make trips to deep environments to feed on demersal fish (hakes, trichiurids, redfish, lanternfish and fish from the Gonostomatidae fam.). Juvenile swordfish do not reach the same depths as adults, so they do not feed demersal fish at great depths (Nakamura, 1985; FAO, 2024). While in shallow waters they prey mostly on neritic pelagic fish such as mackerels, herrings, anchovies, sardines, and needlefish (Nakamura, 1985; FAO, 2024).

1.4 *Reproduction*

Xiphias gladius is a gonochoric and iteroparous species, female and male specimens do not present clear secondary sexual characteristics except for the

body size which tends to be higher in females compared to males (Gioacchini et al., 2019; ICCAT, 2023; FAO, 2024). In mature males, the testicles are elongated, flattened, and ribbed, with spermatocysts at different stages of development distributed along the lobular ribbed zone (Wootton and Smith, 2015). In mature females, the two ovaries are elongated organs located in the center of the abdominal cavity. They are asynchronous, containing oogonia and oocytes at different stages of development. During development, ovaries reach the dimension of half or more than half of the abdominal cavity while changing volume and color based on the different stages of the reproductive cycle (Marisaldi, 2021).

The size and age at which swordfish reach sexual maturity change among different geographical areas. In the Atlantic Ocean, most data concerning sexual maturity are on females, this is because the male sex is often unrecognized and classified as “undetermined” during the sampling activities (Saber et al., 2020). So, no information on Atlantic swordfish male’s L_{50} is reported (ICCAT, 2023). In the Eastern Atlantic, data from 2020 show that 50% of swordfish mature females (L_{50}) have been observed at a length of about 170-180 cm of LJFL (Lower Jay Fork Length) (Figure 6), corresponding to specimens ~5 years old (ICCAT, 2023). From data collected over the years, it appears that in the Atlantic Ocean swordfish reach sexual maturity at greater

length and age compared to the population analyzed from the Mediterranean Sea (Marisaldi, 2021). In the Mediterranean Sea, data from 2018 show that sexually mature males have been found at about 90 cm LJFL (ICCAT, 2023). In the Western Mediterranean, mature females as small as 110 cm of LJFL have been observed and the L_{50} calculated is 142,2 cm (Figure 6) corresponding to an age between 2 and 3,5 years old (ICCAT, 2023). However, different values were also reported, especially from the Western Mediterranean area, where an L_{50} of ~140 cm and 170 cm (LJFL) (Figure 6) were reported in the Southwestern Mediterranean Sea and the Strait of Gibraltar respectively (Macías et al., 2005; Abid et al., 2019; Marisaldi, 2021). In the Central Mediterranean, the L_{50} was calculated by different research groups obtaining values ranging between 131,5 and 134,3 cm (LJFL) corresponding to an age of ~3 years old (Marisaldi et al., 2020, Alıçlı et al., 2012; Akyol & Ceyhan, 2013 and Saber et al., 2020). In the Easter Mediterranean, there are no studies investigating swordfish's L_{50}.

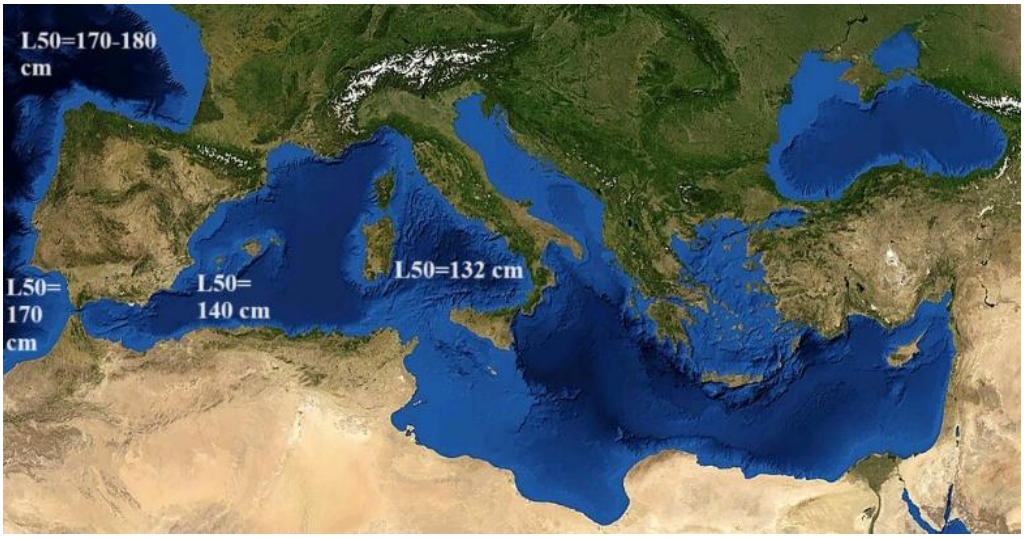

***Figure 6**: female swordfish L_{50} in the Mediterranean Sea and Eastern Atlantic.*

During the reproductive period, mature specimens can release gametes several times into the pelagic environment, for this reason, the swordfish is considered a multiple spawner with external fertilization (Gioacchini et al., 2019). Parental care is not provided, therefore embryonic development is rapid, and hatching occurs two or three days after fertilization (Palko et al., 1981). The dimension of the larvae at the hatching is about 4 mm and during the early stages of life they live near the surface feeding on plankton (Palko et al., 1981).

The reproductive period of the swordfish occurs at different times of the year according to the environmental parameters characterizing different geographical areas. In the Atlantic Ocean, spawning events occur in the Caribbean, the Gulf of Mexico and Florida, with a peak between April and September (Hazin et al., 2002). In the Central Pacific, spawning events occur

during spring from March to July, in the Southwestern Pacific from September to December while swordfish can reproduce all year long in the Equatorial Pacific (Young et al., 2003). In the Indian Ocean, near the island of La Réunion, spawning events take place between October and April (Poisson & Fauvel, 2008). In the Mediterranean Sea, spawning events occur during the summer with a peak in July (Romeo et al., 2009) and the main spawning areas are in the waters west of Sicily, the Strait of Messina, the Strait of Gibraltar, the Balearic Islands and the Levantine Sea (Corriero et al., 2004, Abid et al., 2016; Alıçlı et al., 2012). Differences observed in both reproductive periods and L_{50} values could be explained by the genetic isolation of swordfish populations in different geographical areas. It has been proposed by different researchers that the Mediterranean stock is genetically isolated from the Atlantic stock, and it shows differences in L_{50} (Bremer et al., 2007; Kasapidis et al., 2008; Smith et al., 2015). On the other hand, Righi et al., (2020) investigated microsatellites DNA showing mixing between the Mediterranean and North Atlantic stocks due to the presence of three genetically mixed groups and a high level of admixture within the Mediterranean Sea. In conclusion, information on stock mixing and boundaries is still uncertain, officially three separate stocks are considered: the North and South Atlantic stocks separated at the 5°N and the Mediterranean stock separated from the others by the Strait of Gibraltar (ICCAT, 2023).

1.5 *Fishing and stock management*

Since the 1950s, the most common fishing techniques used to catch swordfish are surface longlines and gillnets (ICCAT, 2023). Since 1999, the mesopelagic longline gears, operating at 100-600 m depth, have been gradually introduced and nowadays they have partially replaced the surface longline gears in several Italian, French, and Spanish swordfish fleets (ICCAT, 2023). Since 2003, the gillnets have been gradually eliminated. A minor portion of catches is reported from harpoon, traps and fisheries targeting other large pelagic species (ICCAT, 2023). All information is stored in fisheries reports of an international commission for the management of pelagic species, known as the "International Commission for the Conservation of Atlantic Tunas" (ICCAT). The ICCAT is a regional fishery management organization responsible for the management and conservation of tuna and tuna-like species, such as swordfish, in the Atlantic Ocean and the Mediterranean Sea. This organization was established in 1966 to compile fishery statistics from all the member states and the entities fishing for these species in the Atlantic Ocean. It coordinates different research projects, including stock assessment, developing scientific-based management advice to provide a mechanism for Contracting Parties to agree on management measures. The Standing Committee Research and Statistics (SCRS) is one of the 14 Cooperating Non-Contracting Parties (CPCs)

that form the international commission. It is responsible for developing and recommending to the entire Commission all policies and procedures for the collection, compilation, analysis, and dissemination of fishery statistics. The SCRS coordinates various national research activities, developing plans for special international cooperative research programs, SCRS carries out stock assessments and advises the Commission on the need for specific conservation and management measures (ICCAT, 2023). The most recent data of stock assessment were obtained for the North and South Atlantic swordfish stocks by SCRS in 2022, using available data up to 2020, while the most recent assessment of the Mediterranean swordfish stock was conducted in 2020 using the available data through 2018 (ICCAT, 2023). The results obtained from these data collection and analysis campaigns revealed different situations among the stocks observed.

1.5.1 *The North Atlantic stock*

Based on results from the 2022 stock assessment, the North Atlantic swordfish stock did not appear overfished before 2022, nor the stock is experiencing overfishing at the moment, representing a healthy stock (ICCAT, 2023).

The stock biomass of the North Atlantic swordfish was above the Maximum Sustainable Yield (B_{MSY}) (estimated at 12819 t) which represents the biomass level that must be maintained to avoid population collapse and the stock

biomass that would provide the highest long-term average catch to the fishery (ICCAT, 2023). The mortality due to fishing activities was below the Maximum Sustainable Yield (F_{MSY}) which indicates the highest possible annual catch that can be sustained by the stock over time (ICCAT, 2023).

Data history regarding the North Atlantic landings highlighted the highest peak of catches in 1987 with 20238 t. In the past decades, the estimated catch of North Atlantic stock showed an average decrease starting from 1987 reaching values around 10400 t per year considering both landings and dead discards. The last data collected confirmed the average values observed in the previous years indeed, in 2022, the swordfish landings were 10349 t (Figure 7) (ICCAT, 2023).

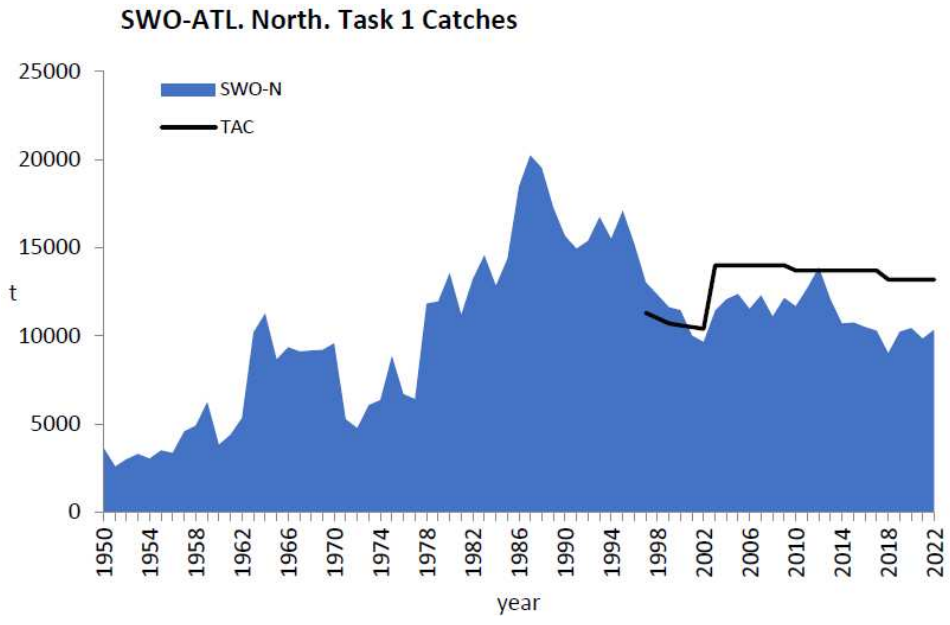

***Figure 7**: North Atlantic swordfish catches (SWO-N) and Total Allowable Catch (TAC) (t, tons of landings and dead discards) from 1950 to 2022 (ICCAT, 2023).*

These reductions in landings have been attributed to ICCAT management measures and to the shifts in fleets distribution including the movement of some vessels to the South Atlantic or out of the Atlantic (ICCAT, 2023). The management measures currently adopted in the North Atlantic consist of a fixed total catch limit of 13200 t and a minimum landing size of 125 cm (LFLJ) and 25 Kg. For eviscerated fish, the landing size limit of 63 cm is calculated from the cleithrum to the keel length (ICCAT, 2023).

1.5.2 *The South Atlantic stock*

The historical trend of catches, in south Atlantic waters, can be divided into two periods: before and after 1980. The first period is characterized by relatively low catches, generally less than 5000 t per year. After 1980, catches increased continuously reaching a peak of 21931 t in 1995. In part, this increase in landings was due to the above-mentioned progressive shifts of fishing efforts from the North to the South Atlantic. The expansion of fishing activities by southern coastal countries, such as Brazil and Uruguay, also contributed to this increase in catches (ICCAT, 2023). After the peak of 1995, catches showed a consistent decrease reaching 8743 t in 2022 (60% lower than the peak of 21931 t) (Figure 8) (ICCAT, 2023).

To date, from data obtained within the 2022 stock assessment, the South Atlantic swordfish stock appeared overexploited (the biomass level is not sustainable due to overexploitation of the stock biomass over time), and overfishing is occurring (ICCAT, 2023). These conditions do not represent a healthy stock (ICCAT, 2023). Indeed, the stock biomass of the South Atlantic swordfish was below the Maximum Sustainable Yield (B_{MSY}) that was estimated at 11481 t while the mortality due to fishing activities was marginally above the Maximum Sustainable Yield (F_{MSY}) (ICCAT, 2023).

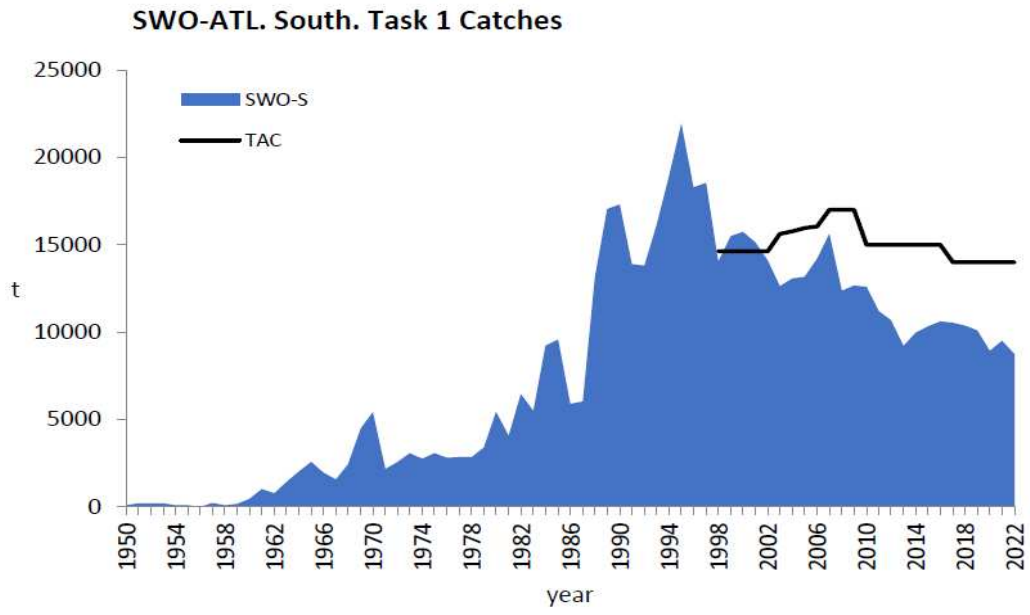

***Figure 8**: South Atlantic swordfish catches (SWO-S) (t, landings, and dead discards) and Total Allowable Catch (TAC) (t) for the period 1950-2022 (ICCAT, 2023).*

This scenario could suggest the necessity to reevaluate the adopted management measures which fix the total catch limit at 14000 t, a minimum landing size of 125 cm (LFLJ) and 25 Kg (ICCAT, 2023).

1.5.3 *The Mediterranean stock*

The stock biomass of the Mediterranean swordfish stock started to decline from 1970 onwards, while the fishing mortality started to exceed the F_{MSY} in the late 1980s when catches peaked. From 1989 up to 2011, the reported landings of swordfish have declined, fluctuating mostly between 12000 to 17000 t. In the early 1990s, the stock became overfished following the full development of the fishery. Since 2018, the overall fishing effort has been decreasing with catches below 10000 t (Figure 9) (ICCAT, 2023).

Based on results from the 2022 stock assessment, the Mediterranean swordfish stock is now considered overfished (the biomass level is not sustainable due to overexploitation of the stock biomass over time), but overfishing is not occurring (the fishing effort is sustainable, although it is at the limits of sustainability). However, the population does not reflect a healthy stock (ICCAT, 2023).

Anyway, all this data may not represent the real situation due to the low percentage of fleets that provide information on their annual dead discards. The consequent biased stock assessment could present a more favorable situation than the actual one. For this reason, ICCAT continues to express concerns about the lack of collaboration by fishermen (ICCAT, 2023).

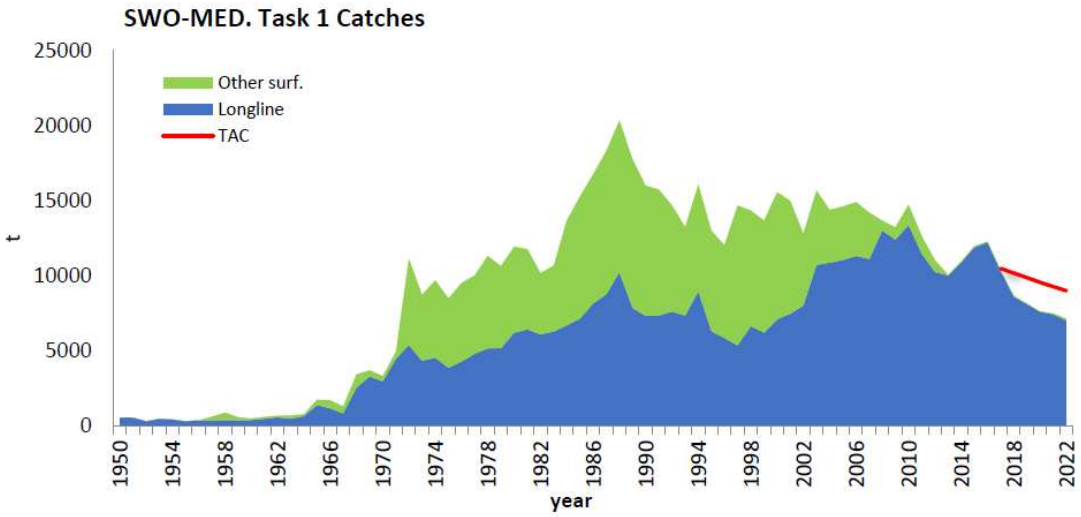

***Figure 9**: estimates swordfish catches (in tons) in the Mediterranean Sea for the period 1950-2022 and corresponding annual TACs since 2017 (ICCAT, 2023).*

Management measures adopted by ICCAT for the Mediterranean swordfish stock consisted of imposing a total catch limit of 10500 t in 2017 (with a 3% annual reduction over the period 2018-2022), a three-month fishery closure (from 1 October to 30 November and during an additional period of one month between 15 February and 31 March or during the period from 1 January to 31 March each year), limiting the number and size of hooks (maximum 2500 hooks always bigger than 7 cm of height) (ICCAT, 2023). Also, the length of the gear was regulated (maximum 30 NM/55 km) and the minimum catching size (that recently increased from 90 to 100 cm resulting in discard increases up to 600% or in alternative less than 11,4 kg of round weight or 10,2 kg of gilled and gutted weight). A list of authorized vessels, fishing capacity restrictions and domestic observers onboard longlines vessels targeting

Mediterranean swordfish have been adopted to monitor the situation (ICCAT, 2023).

It appears quite clear the necessity to increase the effectiveness of management measures to ensure proper exploitation of this high-value species without affecting the stability and the health status of the population. To reach this objective, it is necessary to develop a strong knowledge of population dynamics and reproduction (Gioacchini et al. 2019). For instance, both size and age of first sexual maturity are key information for the stock assessment, but accurate scientific methods to provide them have not been developed yet. This means that management measures based on uncertain data may be vain or less effective than they should be.

However, some general and uncertain information exists about swordfish reproduction, such as reproductive periods and breeding grounds for different populations (Abid et al., 2019; Gioacchini et al., 2019; Saber et al., 2020; Marisaldi, 2021). Unfortunately, all this information is not considered yet in fishery management. For example, in the Mediterranean Sea swordfish reproduce in summer, but fishery activities are halted in winter following the ICCAT directives. It is clear that the measure does not follow sustainability principles, not allowing the regeneration of the resource and the perpetuation of the species over time. The stock management and conservation of the species

result extremely complicated, due to unsolved gaps of knowledge about the species' reproduction pattern and because of management measures that do not follow scientific advice.

1.6 *Swordfish Year Programme*

In the last few years, a step forward to improve the management of swordfish based on scientific evidence associated with data collected from the market has been made with the Swordfish Year Programme (SWOYP). It was established in 2018 to address key uncertainties in stocks management and in 2022, it was formalized as an ICCAT research program. SWOYP involves 21 institutions and 14 Cooperating Non-Contracting Parties (CPCs). Within SWOYP, the SCRS focuses on three main research areas: ageing and growth, reproductive biology, and genetics. Each of the three research areas is overseen by project leaders: ageing and growth (Dr. Rui Coelho and Ms. Daniela Rosa, Instituto Português do Mar e da Atmosfera (IPMA)), reproduction (Dr. David Macías (Instituto Español de Oceanografía (IEO)) and genetics (Dr. Oliana Carnevali and Dr. Giorgia Gioacchini (Università Politecnica delle Marche) (UNIVPM) (ICCAT, 2023). Since project inception, 4647 swordfish representing the three ICCAT-managed stocks (North, South Atlantic and Mediterranean Sea) have been sampled for fin spines, otoliths, muscle tissue and gonads. Additional information has been collected on fish size, sex, and stage of sexual maturity.

The SWOYP aims to improve knowledge of the stock distribution, the age and sex of the catch, the growth and maturation rates, the age of first sexual maturity, the season and location of the spawning, the stock boundaries and mixing. In addition, tagging work supports studies on distribution, movement and habitat use which are important for the development of a species distribution model. Since 2019, the analysis of samples has permitted to the improvement of knowledge on the ageing and sexual maturity of swordfish (ICCAT, 2023). Genetic analyses led to the sequencing of the swordfish genome, the identification of Single-Nucleotide Polymorphisms (SNPs), important for stock differentiation, and the preliminary estimates of stock boundaries and mixing areas. This program is still active in 2024 through the analysis of otoliths/spines and gonads samples, genetic analysis, and collection of samples in areas with low or lack of information (ICCAT, 2023). For the ageing purpose, the ICCAT collected a total of 3535 spines and 1352 otoliths from the North and South Atlantic and the Mediterranean Sea: 1093 spines and 344 otoliths were collected for the North Atlantic swordfish; 979 spines and 511 otoliths were collected in the South Atlantic swordfish; 173 spines and 50 otoliths were collected in the Mediterranean Sea (ICCAT, 2023). The aims of the ageing studies are to develop a standardized methodology using spines and

otoliths to age the swordfish and validate ages through alternative procedures such as bomb radiocarbon and epigenetic (ICCAT, 2023).

1.7 *Age determination: the swordfish case*

The age determination of specimens within a population provides essential information useful for an effective management plan.

Data collected from 1983 to 1999 estimated that over one million fish were aged worldwide (Campana and Thorrold, 2001). Knowing the age of a representative subsample of a population allows generating a growth curve to assess over time the variability of the growth rate (NIWA, 2012). Moreover, it is possible to calculate the mortality rate by evaluating the decrease in the frequency of fish in each year class (NIWA, 2012). Age information is essential to rebuild the age structure of a population and to determine the most exploited age class (corresponding to the less represented age class) (NIWA, 2012; Anastasiadi & Piferrer, 2022).

In cases where age information is not available, it may be possible to estimate the age indirectly. For instance, by sampling individuals and measuring their length, age can be estimated based on the species' growth rate, but only if age-length relationships have already been validated (Campana, 2001). Age estimation in fish has traditionally relied on analysis of growth marks in hard

structures (such as vertebra, scales and otoliths) in an analogous manner that trunk rings are used to estimate the age of trees (Campana and Thorrold, 2001).

The accurate estimation of *Xiphias gladius*'s age is critical, as well, to properly understand the dynamics and health of the stocks (Millot et al., 2024). In general, traditional methods to determine the fish age are time-consuming, often lethal, of low accuracy in some species and require well-trained personnel (Campana and Thorrold, 2001). Swordfish age determination is extremely hard due to different challenges such as the collection of adequate samples' number for each age, the dissection and the conservation of samples on board. Most age analyses are performed on different bony tissues such as anal-fin rays, otoliths, and vertebrae (Esteves et al., 1995; Ehrhardt et al., 1996; Uchiyama et al., 1998 and DeMartini et al., 2007). The choice of one bony structure over another depends on sample conditions before the reading and on the operators' experience (Casselman, 1983; Prince et al., 1988; Esteves et al., 1995).

1.7.1 *Fin-ray analysis*

The officially accepted protocol to analyze fin-ray follows the method proposed by Young and Drake (2003). Other protocols that can be used are by Tserpes and Tsimenides (1995) and Ehrhardt et al. (1996). They consist of the measurement of the distance from the core to the most external part of the section of the fin ray and between every annual increment within the section.

Typically, thin translucent bands and wide opaque bands appear alternated outwards from the center to the edge of the section, each alternation corresponds to a year of age (Figure 10) (Millot et al., 2024).

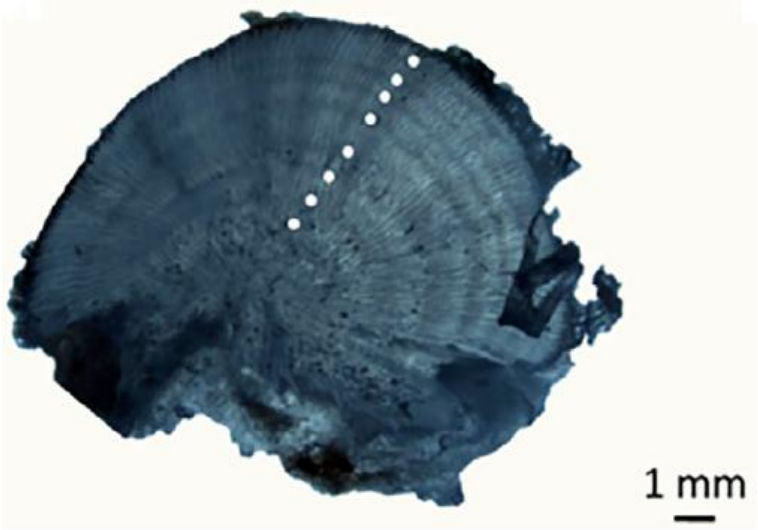

Figure 10: *transverse section of swordfish fin ray. Each white dot corresponds to one year of age (Millot et al., 2024).*

The fin-ray analysis is the most used method for age estimation. The fins are easily sampled without impacting the economic value of the fish (Quelle et al., 2014). However, 10-15% of fin sections are discarded due to the vascularity and the resorption which cause the loss of annual increments (Sun et al., 2002; Farley et al., 2022). To minimize this problem, Tserpes and Tsimenides (1995) proposed to combine several techniques to reduce the age error induced by rings' loss. Farley et al. (2022) and Nishimoto et al. (2006) also found that age estimation errors often occur at 4 years for males and 7 years for females, so

the error increases with the aging of the fish, in fact, the fin-ray method is more reliable for swordfish under 6 years old (Millot et al., 2024).

1.7.2 *Otolith analysis*

Another way to determine the swordfish age is represented by the otoliths analysis (Millot et al., 2024).

On both sides of the swordfish head, there are two optic capsules from which three pairs of otoliths (sagittae, lapilli, asterisci) can be extracted. For aging purposes, sagittal otoliths are the pair that is usually analyzed with two different techniques. The first one consists of the whole sagittal otolith examination, while the second method analyzes the transversal section of the otolith. For the first technique, the annual increment is enumerated from the core to the rostrum (ventral direction) or along the antirostrum (dorsal direction) depending on the ring visibility, so each ring corresponds to one year of age (Figure 11) (Millot et al., 2024).

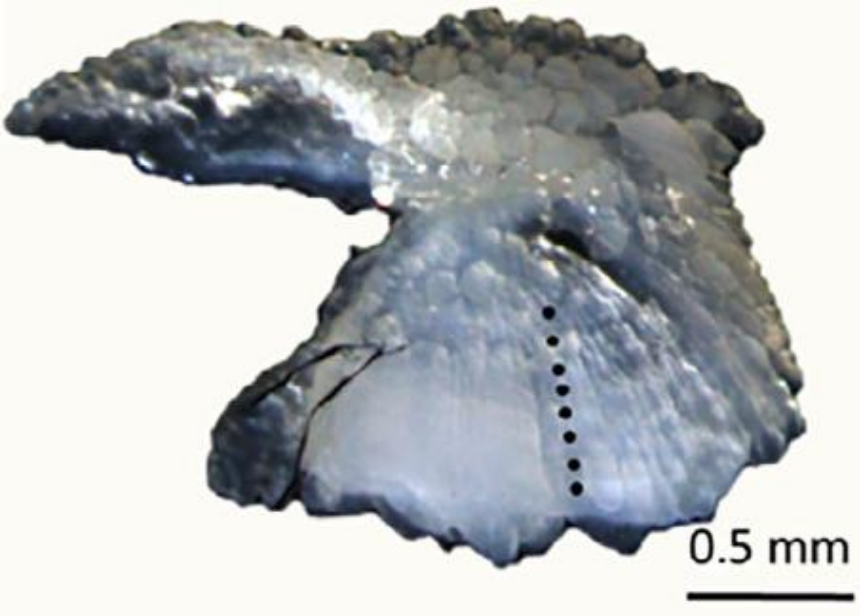

Figure 11: *image of a swordfish sagittal otolith. Each black dot corresponds to one year of age (Millot et al., 2024).*

For the second technique, sagittal otoliths are sliced into 200–250 µm thick transverse sections in a four steps procedure following the Robertson and Choat (2002) protocol. Two measurements are taken: the distance from the core to the edge of the otolith section (otolith radius) and from the core to the edge of the first annulus. From sagittal sections, otolith annuli are enumerated according to Farley et al. (2022) (Figure 12) (Millot et al., 2024).

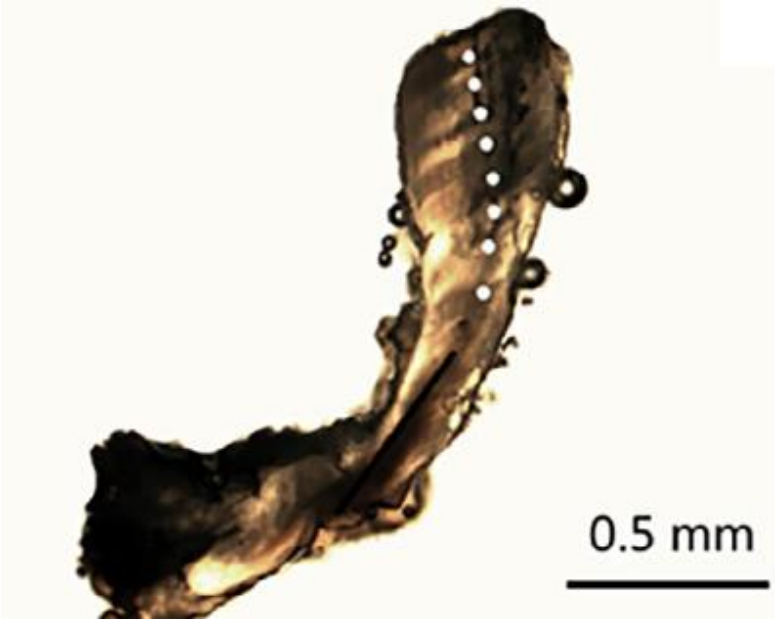

Figure 12: *transverse section of a swordfish sagittal otolith. Each white dot corresponds to one year of age (Millot et al., 2024).*

Among existing age estimation techniques, the use of otoliths is the most time-consuming method regarding sample preparation. Otoliths are difficult to extract, and they can be damaged during this process (Millot et al., 2024). 33-64% of otoliths are commonly lost or damaged and therefore discarded (Wilson & Dean, 1983; Esteves et al., 1995). Nevertheless, the otolith section used for aging fish is rarely unreadable (Nishimoto et al. 2006; Farley et al. 2022). In contrast, the percentage of whole otoliths reported as unreadable is much greater, and it is the least reliable technique for the age estimation of swordfish (Millot et al., 2024). Indeed, Esteves et al. (1995) found 10,6% unreadable otoliths due to difficulties recognizing the annuli.

1.7.3 *Vertebrae analysis*

The age estimation based on vertebrae analysis considers most anterior vertebrae (1 to 5) which are extracted from the occipital cranial region. Usually, the third vertebra is the easiest to read and, therefore the most used (Millot et al., 2024). The surface of the vertebral cone is characterized by annual growth zones, an alternate pair of opaque and translucent bands which is counted as one year of age (Figure 13) (Millot et al., 2024).

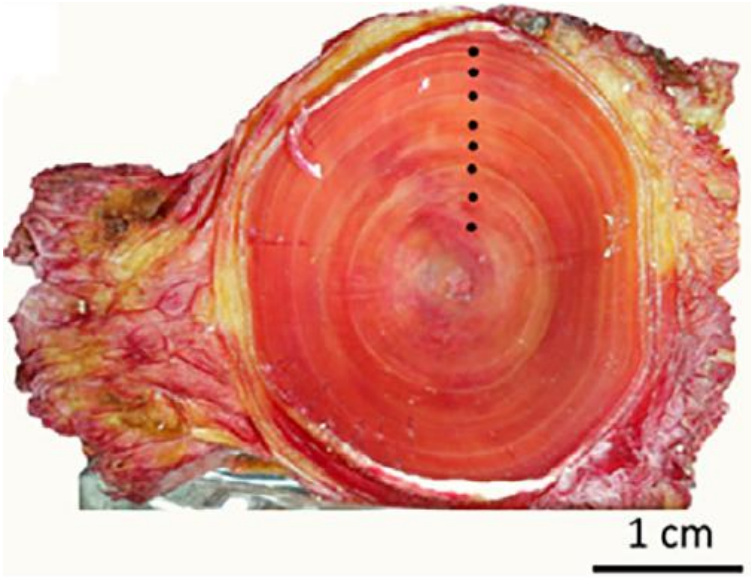

***Figure 13**: transversal section of a third swordfish vertebral cone. Each black dot corresponds to one year of age (Millot et al., 2024).*

This method is the least efficient since vertebrae preparation is time-consuming and age estimation appears difficult. Annual increments are hard to distinguish, and they can be confused with other marks (Millot et al., 2024). On average, around 19% of vertebra samples can be rejected because unreadable (Esteves

et al., 1995). Millot et al. (2024) have reported that readers with poor experience and a small number of samples negatively influence reading results. Moreover, vertebra extraction impacts on the appearance of the fish and consequently their economic value (Millot et al., 2024).

1.7.4 *Age validation methods*

Independently of samples type, different approaches exist to validate age readings obtained from otoliths, vertebrae or anal fin such as the radiocarbon chronometer technique based on the measurement of C^{14} content in organic material; the tag-recapture method to mark a sample of individuals, releasing them, and then recapturing another sample calculating its age; the characterization of the chemical composition of otoliths involving the analysis of the isotopic and chemical composition of these hard parts, as otoliths accumulate material during the growth, variation in their composition can provide insights into the individual's life history and age (Kalish et al., 1996, Heimbrand et al., 2020 and Hüssy et al., 2021). These methods are not yet fully valid, and their application may lead to inaccurate results. For radiocarbon chronometer: the method is only effective for organic materials up to 50000 years old; sample contamination can alter C^{14} measurements and fluctuations in atmospheric C^{14} levels can affect accuracy (Campana et al., 1997). For the recapture method: it is assumed that the population is closed unrealistically;

some individuals may be more susceptible to capture and the time between marking and recapture must be adequate (Pine et al., 2003). For the chemical characterization of otoliths: differences in diet and growth may affect the chemical composition of otoliths and require sophisticated equipment, moreover, information obtained may be complex and may require expert interpretation (Campana et al., 1999). For all the reasons just explained above, today the SWOYP project is trying to obtain a standardized protocol for the age validation of the swordfish looking further for new valid methods, especially based on epigenetic (ICCAT, 2023).

1.8 *Epigenetic and epigenetic clock*

Epigenetics can be defined as the change in gene expression and phenotype due to changes not affecting nucleotide sequences. These changes are heritable during mitosis and meiosis events; therefore, they pass from parents to their offspring (Deans and Maggert, 2015). One of the main epigenetic mechanisms for the regulation of gene expression is DNA methylation (Brock and Fisher, 2005). Specifically, DNA methylation is a chemical modification of the DNA, where the 5' carbon atom of cytosine is modified by the addition of a methyl group (CH_3), becoming 5'-methylcytosine (Hermann et al., 2004). DNA methylation only occurs when cytosine is followed by a guanine and linked by a phosphate bond, so in a CpG (Cytosine-phosphate-Guanine) context

(Hermann et al., 2004). The enzymes, responsible for DNA methylation, are called DNA methyltransferases (DNMTs). For instance, DNMTs are classified according to their targets. DNMT3 methylates previously unmethylated CpGs and is thus responsible for the *de novo* DNA methylation. On the other hand, DNMT1 methylates the unmethylated opposing pair of a hemi methylated site. DNMT1 is called maintenance DNMT, because is responsible for copying the existing methylation profile during cell division and, thus, participates in the transmission of epigenetic marks and contributes to the epigenetic inheritance mechanism (Hermann et al., 2004).

In the genome, CpGs are usually methylated and evenly distributed, except in regions where they are more concentrated. These regions are called CpG islands (CGIs), they are normally associated with promoter or regulatory regions and their methylation levels are associated with the regulation of gene expression (Jung & Pfeifer, 2015). The variation in the DNA methylation level is influenced by intrinsic, extrinsic factors and stochastic events. For instance, DNA methylation changes are associated with aging (Jung & Pfeifer, 2015). There is an age-dependent change in DNA methylation that may be summarized in the global genomic hypomethylation followed by the hypermethylation of specific CpGs (Heyn et al., 2012). This DNA methylation change is defined as “clock-like”; a clock is structured with fixed numbers and

moving hands, in this model the CpGs loci represent the numbers, therefore the reference points, and the levels of methylation represent the clock hands since they change overtime. For every CpGs locus? There is a specific level of methylation. Knowing this information, it is possible to find a correlation between the level of methylation in specific CpGs and age (De Paoli-Iseppi et al., 2019). For this reason, the chronological age predictors built from DNA methylation are called “epigenetic clocks” (Zhang et al., 2019). To summarize, these types of clocks consider the hypo and hypermethylation level from a group of carefully selected loci to obtain the chronological age of certain species with high precision (Anastasiadi & Piferrer, 2022; Piferrer et al., 2023).

A tissue-independent epigenetic clock was first developed in humans, and it was made of 353 clock CpGs. These CpGs can be divided into two sets according to their correlation with age: 193 positively and 160 negatively correlated CpGs become respectively hypermethylated and hypomethylated with age (Horvath, 2013). Even though recent epigenetic clocks have been developed for mammals (Lu et al., 2021) and fish (Mayne et al., 2020), further studies are important for the normalization of the methods on a wider range of animal species, especially on those endangered or subject to improper management.

1.9 *Sequencing in the epigenetic clock development*

This section illustrates the sequencing technologies to quantify methylation changes in the development of epigenetic clocks with a specific focus on the main used experimental techniques.

Sequencing is a technology that allows for the analysis and determination of the nucleotide sequence in DNA or RNA (Metzker, 2010), also used to analyze the genetic structures related to aging, such as CpG islands. Notable examples of these employed technologies include microarray (Horvath, 2013), pyrosequencing (Polanowski et al., 2014), Digital Restriction Enzyme Analysis of Methylation (DREAM) (Jelinek et al., 2016), Multiplex Bisulfite Sequencing (MBS) (Anastasiadi & Piferrer et al., 2020) and Reduced Representation Bisulfite Sequencing (RRBS) (Thompson et al., 2018). The latter three techniques rely on Next-Generation Sequencing (NGS), which allows the parallel sequencing of millions of DNA fragments, offering an accurate assessment of methylation levels across the genome (Behjati & Tarpey, 2013).

1.9.1 *Microarray*

Microarrays, one of the first technologies used for the development of epigenetic clocks, are sophisticated and widely used tools for evaluating gene

expression (Stears, 2003) as well as methylation patterns across the genome (Horvath, 2013).

Using this technology, Horvath (2013) developed an epigenetic clock in humans. Specifically, the extracted DNA was labeled with fluorescent dyes and applied to a microarray platform containing probes that bind to specific CpG sites. Upon binding, the light was emitted (Horvath, 2013). The intensity of the emitted light was proportional to the methylation level at each CpG site, providing a means to quantify methylation and estimate biological age (Horvath, 2013; Garma et al., 2024). The results were then analyzed using bioinformatics software ultimately leading to the development of the epigenetic clock (Horvath, 2013).

As demonstrated by the study of Horvath (2013), the technique can be used for the development of epigenetic clocks, but it has a major limitation since it targets only a few CpG sites, providing an extremely limited genome coverage. This means that important genomic information may be missed during analysis (Horvath, 2013). To develop an accurate and functional epigenetic clock, complete data on methylation levels of a wide range of CpGs across the genome is needed. So, the microarray does not provide the completeness required (Garma et al., 2024).

As a result, more advanced techniques with broader genomic coverage and higher resolution will be necessary to improve the reliability and accuracy of epigenetic clocks.

1.9.2 *Pyrosequencing*

After examining the application of microarrays and their challenges in the development of the epigenetic clock, another used technique is pyrosequencing.

Pyrosequencing is a DNA sequencing method that measures the emitted light when a new nucleotide is incorporated into the growing DNA strand, allowing the detection of the nucleotide order (Ronaghi, 2001). This technique can also be used to study methylation levels across the genome. In fact, pyrosequencing was employed in the study by Polanowski et al. (2014) to develop an epigenetic clock.

In this study, the extracted DNA was treated with bisulfite, which converts unmethylated cytosines into uracil, while methylated cytosines remain unchanged (Polanowski et al., 2014; Beck et al., 2022). After this treatment, specific CpG regions were amplified using PCR. The resulting amplicons were analyzed by pyrosequencing, enabling the real-time detection of the emitted light, with its intensity directly proportional to the methylation levels (Polanowski et al., 2014). During this process, unmethylated cytosines

(converted to uracils) were read as thymine (Polanowski et al., 2014; Beck et al., 2022). The sequencing results were analyzed using bioinformatics tools to develop the epigenetic clock (Polanowski et al., 2014).

As demonstrated in the previous study, pyrosequencing can be applied to epigenetic clocks' development. However, while it detects methylation at a few CpG sites with high sensitivity, it fails to capture a broader range across genomic regions (Polanowski et al., 2014; Ghemrawi et al., 2023). As a result, it does not provide the extensive data required for developing a precise and functional epigenetic clock (Garma et al., 2024).

In conclusion, this technique will need to be integrated with more advanced approaches, such as next-generation sequencing, which allows for a more comprehensive view of genomic methylation.

1.9.3 *Digital Restriction Enzyme Analysis of Methylation (DREAM)*

While pyrosequencing offers high sensitivity at a single CpG level, it still presents limitations. A promising technique called Digital Restriction Enzyme Analysis of Methylation (DREAM) has emerged.

DREAM is a method that allows the investigation of methylation levels across the genome through specific enzymes (Jelinek et al., 2016; De Paoli-Iseppi et al., 2019).

In the study by De Paoli-Iseppi et al. (2019), DREAM was used to develop an epigenetic clock for a seabird species. After DNA extraction, samples were treated with restriction enzymes that target age-associated CpG sites. These were amplified through PCR. The amplicons were analyzed using NGS, and the results were subsequently processed with bioinformatics tools to develop the epigenetic clock (De Paoli-Iseppi et al., 2019).

The study demonstrates that the DREAM method can be utilized in epigenetic clocks' development by targeting a specific subset of CpG sites with specialized enzymes. While this specificity can be beneficial, it also means that DREAM may overlook important age-associated CpG sites or genomic regions, limiting its effectiveness (Garma et al., 2024). Furthermore, the enzymes used in DREAM are highly sensitive to the quality and quantity of the DNA, making it challenging to apply in cases of low-quality samples (De Paoli-Iseppi et al., 2019).

Thus, while DREAM offers some advantages, it does not overcome the limitations of other techniques, such as microarrays (Horvath, 2013) and pyrosequencing (Polanowski et al., 2014) and may not be the most effective method for developing an epigenetic clock.

1.9.4 *Multiplex Bisulfite Sequencing (MBS)*

Multiplex Bisulfite Sequencing (MBS) overcomes limitations of microarrays, pyrosequencing, and DREAM, providing a more comprehensive approach to epigenetic clock development.

MBS is an advanced sequencing technique used to investigate methylation levels over the genome (Anastasiadi & Piferrer, 2020).

It was used by Anastasiadi & Piferrer (2020) to select entire regions of CpG sites along with their methylation levels to develop an epigenetic clock for the European seabass. In this study, DNA was extracted and treated with sodium bisulfite. Afterward, the DNA was amplified through PCR using primers targeting specific CpG regions. The resulting amplicons were sequenced using next-generation sequencing (NGS) to study methylation levels in the selected regions (Anastasiadi & Piferrer, 2020). The sequencing data were subsequently analyzed using bioinformatics tools to identify age-associated methylation patterns and develop the epigenetic clock (Anastasiadi & Piferrer, 2020).

While MBS can be used in the epigenetic clocks development, covering entire CpG genomic regions, the risk of selecting irrelevant or less informative regions for analysis is a key limitation (Anastasiadi & Piferrer, 2020). Including CpG regions whose methylation levels are not linked to aging can compromise

the accuracy of the epigenetic clock, leading to inconsistent results (Anastasiadi & Piferrer, 2020).

In conclusion, although MBS improves on earlier techniques, it is not a fully reliable solution for developing highly accurate epigenetic clocks (Anastasiadi & Piferrer, 2020; Garma et al., 2024). Techniques that ensure the inclusion of relevant age-associated regions should be prioritized (Gu et al., 2011).

Despite its challenges, MBS represents an improvement over previous methods, but ongoing development is needed to ensure the selection of genomic regions truly relevant to biological age.

1.9.5 *Reduced Representation Bisulfite Sequencing (RRBS)*

Reduced Representation Bisulfite Sequencing (RRBS) overcomes the limitations of MBS, DREAM, pyrosequencing, and microarray in the development of epigenetic clocks.

RRBS is a sequencing method that uses methylation-sensitive restriction enzymes to fragment the genome at CpG-rich regions (CpG islands), which are known to be closely associated with age (Gu et al., 2011).

RRBS was employed by Michael J. Thompson et al. (2018) to develop an epigenetic clock in mice. In this study, DNA was extracted, digested with methylation-sensitive enzymes and bisulfite-treated. The fragments were

amplified by PCR and sequenced using next-generation sequencing (NGS). The data were then analyzed using bioinformatics tools to construct the epigenetic clock (Thompson et al., 2018).

As shown in this study, RRBS is effective in developing epigenetic clocks due to its targeted approach. By focusing on CpG-rich regions (CpG islands) that are strongly linked to age, RRBS enables the creation of precise epigenetic clocks (Jung & Pfeifer, 2015). Moreover, RRBS excels in tissue specificity and sensitivity, providing valuable insights into age-related methylation changes across various biological samples (Thompson et al., 2018; Beck et al., 2022).

Given the advantages of extensive genome coverage and the focus on CpG sites strongly associated with age, RRBS has emerged as one of the most promising methods for developing accurate epigenetic clocks.

1.9.6 *Whole Genome Bisulfite Sequencing (WGBS) and RRBS*

In addition to RRBS, another technique to consider for epigenetic clock development is Whole Genome Bisulfite Sequencing (WGBS).

WGBS is a sequencing technique that applies bisulphite treatment to the entire genome, followed by the sequencing of the bisulphite-converted DNA. No fragmentation is performed before bisulphite conversion, meaning that the entire bisulphite-converted genome is sequenced (Beck et al., 2022).

When comparing the performances of WGBS and RRBS for developing an epigenetic clock, it is shown that both techniques cover a similar range of CpG sites (Beck et al., 2022). Additionally, both provide approximately 75% genome coverage (Guo et al., 2013). However, none of the two techniques provides a comprehensive examination of methylation patterns across the entire genome (Guo et al., 2013).

Both also face similar alignment challenges during bioinformatics processing, leading to a large proportion of reads that map ambiguously and that will be lost (Guo et al., 2013; Beck et al., 2022).

Although both WGBS and RRBS show comparable performance in terms of CpG coverage, WGBS is less suitable for epigenetic clock development due to its inability to investigate the methylation level of individual CpG sites with the same resolution and sensitivity as RRBS (Beck et al., 2022).

RRBS, by focusing on CpG islands and specific regulatory regions, allows for more targeted, accurate measurements of methylation levels that are closely associated with age (Jung & Pfeifer, 2015).

Furthermore, RRBS offers practical advantages over WGBS. WGBS is computationally intensive and requires higher sequencing costs due to the need to sequence the entire genome, generating large amounts of data that require substantial computational resources for processing (Beck et al., 2022). In

contrast, RRBS reduces both costs and complexity by targeting a smaller subset of the genome, while still providing a high degree of accuracy and sensitivity, particularly for age-related methylation changes (Beck et al., 2022).

Therefore, while WGBS provides a comprehensive approach to methylation analysis, RRBS may be the more suitable sequencing technique for developing a reliable and cost-effective epigenetic clock, particularly for studies where genome-wide data is not required, and cost-efficiency is a priority.

1.10 *Epigenetic clock in fish*

Building upon the techniques discussed earlier, several of these methods have been successfully applied to the epigenetic age determination of fish. This section will examine key studies in this field, starting with model organisms such as zebrafish and expanding to larger pelagic species like tuna. The goal is to underscore the potential of epigenetics as a tool for age determination in commercially valuable fish species, ultimately contributing to the advancement of fisheries management practices.

1.10.1 *The zebrafish case study*

To develop a novel approach for age estimation in fish, Mayne et al. (2020) used zebrafish (*Danio rerio***,** Hamilton, 1822) as a model species to find specific epigenetic biomarkers related to the age of specimens. The zebrafish is a valuable model for vertebrate ageing research due to its low cost of

maintenance, short life cycle, regenerative ability, and senescent phenotype with increasing age (Gilbert et al., 2014 and Gerhard et al., 2003). The zebrafish has a long history as a genetic model organism, with a well-characterized genome that can be genetically manipulated (Kishi et al., 2004; Rafferty et al., 2018 and Keller et al., 2018). The zebrafish's epigenome varies similarly to other species of fish and DNA methylation has a key role in the embryo regulating cell development (Mhanni et al., 2004; Cavalieri et al., 2017).

Mayne et al. (2020) accurately predicted the age of zebrafish through the identification of age biomarkers using the Reduced Representation Bisulfite Sequencing (RRBS) and a known age series. DNA sequencing and statistical analysis were useful to identify 1311 CpG sites significantly correlated to the increase in age. Thanks to additional statistical analysis, 29 CpG sites were identified as the zebrafish's epigenetic clock or age biomarkers. The epigenetic age was determined from the methylation level of these 29 sites and then a high correlation with the known chronological age was observed (Figure 14) (Mayne et al., 2020).

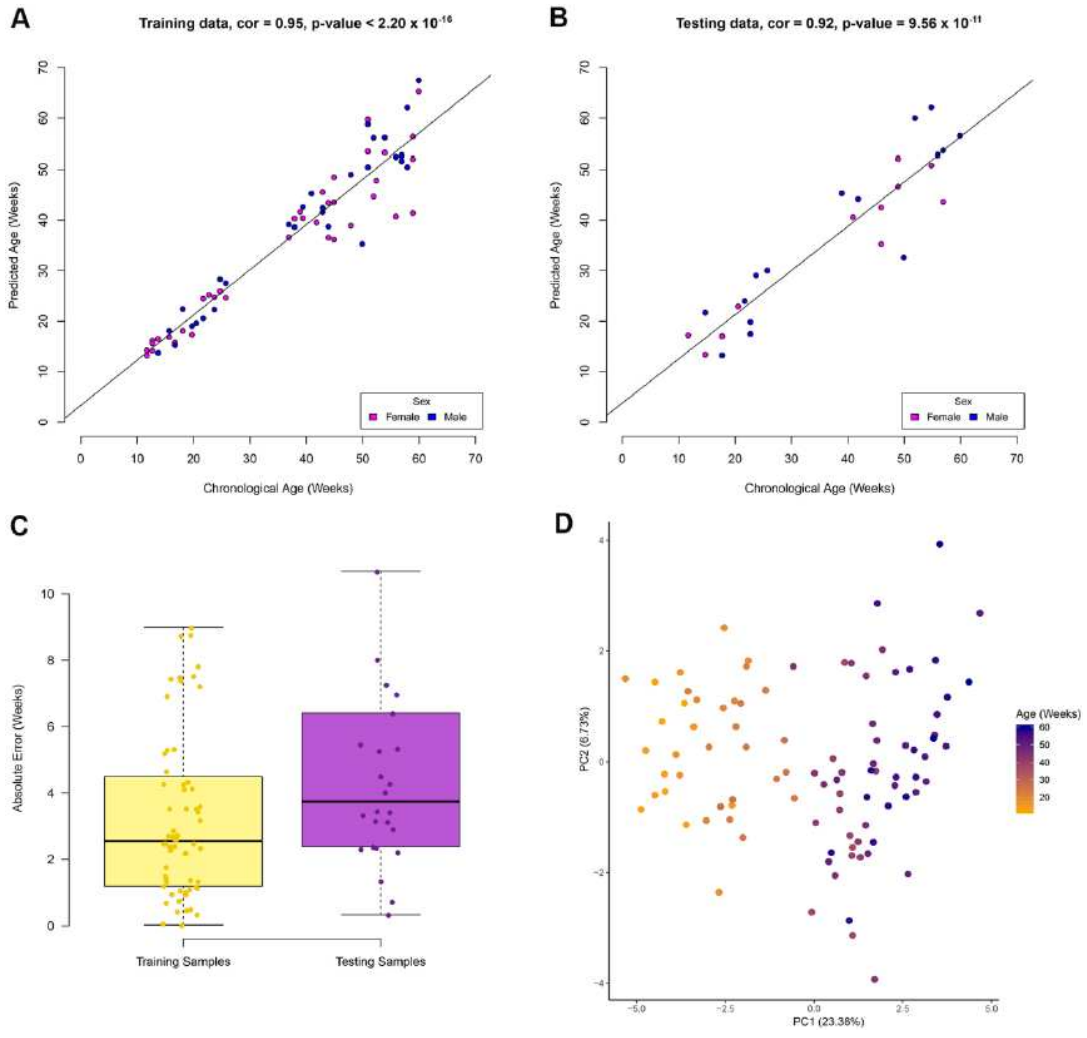

Figure 14*: samples were randomly assigned to either a training or a testing data set to maintain equal ratios of sex in each data set. A high correlation between the chronological and the predicted epigenetic age was observed in: (A) the training data set (Pearson correlation = 0,95; p-value < 2,20x10^{-16}) and (B) the testing data set (Pearson correlation = 0,92; p-value = 9,56x10^{-11}). (C) A median absolute error (MAE) of 3,7 weeks was found. (D) The principal component analysis (PCA) explains 23,4% of the variation by age (Mayne et al., 2020).*

In conclusion, the study of Mayne et al. (2020) is the first to highlight the potential use of DNA methylation as an age predictor in fish (Mayne et al., 2020). This ageing model could be used for commercial or threatened species of fish, and it would be of major significance considering the importance of age

structure for stock management and the lack of effective non-lethal alternatives to estimating the age (Mayne et al., 2020).

1.10.2 *The Southern Bluefin Tuna case study*

Mayne et al. (2020) were also able to determine the age of a species of strong commercial and ecological importance such as the Southern Bluefin Tuna (*Thunnus maccoyii*; Castelnau, 1872). The study in question focused on the pioneer DNA method based on zebrafish's age biomarkers (Mayne et al., 2020). Using muscle tissue, this method was calibrated (89 samples) and tested (36 samples) with ages derived from otoliths (from 1 to 38 years), also using the epigenetic clock derived from the zebrafish (*Danio rerio*) (Mayne et al., 2020). There was a significant statistical correlation between otolith-age and the predicted epigenetic age by DNA methylation (Figure 15), demonstrating that the DNA methylation in Southern Bluefin Tuna is predictive of age (Mayne et al., 2020).

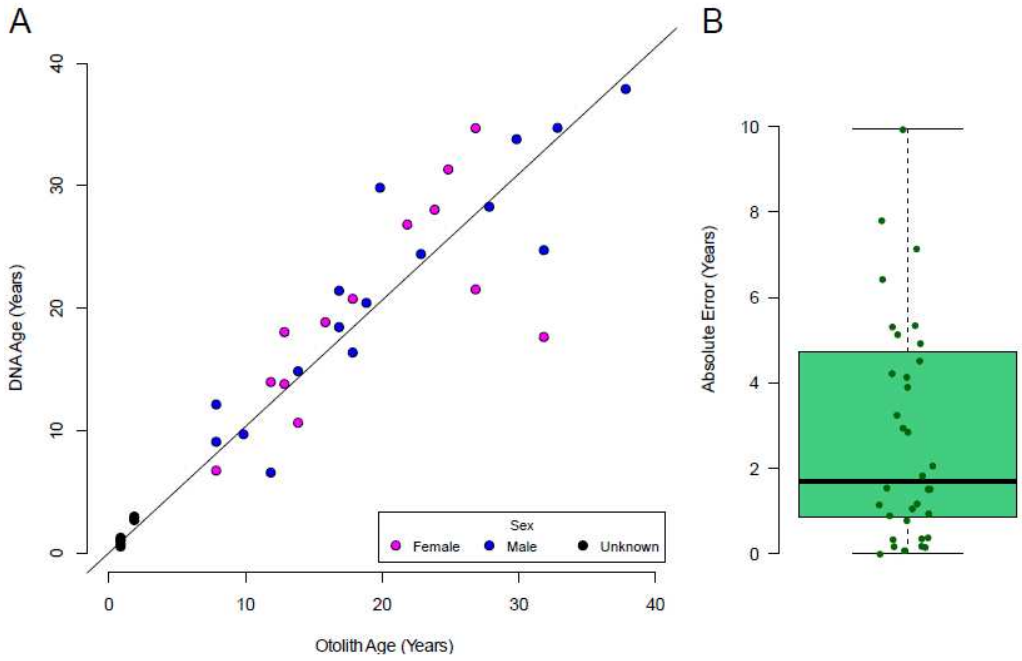

Figure 15: *the performance of age prediction by DNA methylation in Southern Bluefin Tuna. A) The correlation between the age derived from otoliths and predicted epigenetic age (Pearson correlation = 0,93, p-value = 1,23 x 10^{-16}). B) Absolute error rate between the otolith age and the DNA age (Median absolute error = 1,7 years) (Mayne et al., 2020).*

By using DNA age biomarkers from other species of fish, it is possible to potentially develop a universal assay for fish age prediction (Mayne et al., 2020). The limiting factor of the method is the cost of DNA sequencing of wild animals, nonetheless, the model could be improved through additional DNA sequencing to identify other age biomarkers that may increase the accuracy of the method (Mayne et al., 2020).

1.10.3 *The reef fish case study*

The aim of Weber et al. (2022) study is to understand if the epigenetic age determination technique works also without the use of the zebrafish's age

biomarkers (Mayne et al., 2020). These biomarkers are obtained in a controlled environment where fish are not exposed to habitat heterogeneity. For this reason, differences in DNA methylation levels could be present between wild and controlled species (Weber et al., 2022).

On this basis, Weber et al. (2022) have applied the epigenetic age technique to: the red snapper (*Lutjanus campechanus,* Poey, 1860) and the red grouper (*Epinephelus morio,* Valenciennes, 1828) sampled in the Gulf of Mexico. For each species, the age was estimated by counting the otolith sections, in addition, all the red snapper samples had their age validated by the bomb radiocarbon chronometer (Weber et al. 2022).

DNA extraction and RRBS sequencing were used to identify the CpG sites showing a DNA methylation level correlated to age (Weber et al. 2022). For the red snapper, the statistical analysis identified 3224 sites showing age-correlated methylation. More specific statistical analysis retained 199 CpG sites, in the age-predictive model, as the epigenetic biomarkers of the red snapper (Figure 16 A) (Weber et al., 2022). For the red grouper, the statistical analysis identified 690 sites showing significant age-correlated methylation. More specific statistical analysis retained 49 CpG sites in the age predictive model identified as the epigenetic clock of the red grouper (Figure 16 B) (Weber et al., 2022).

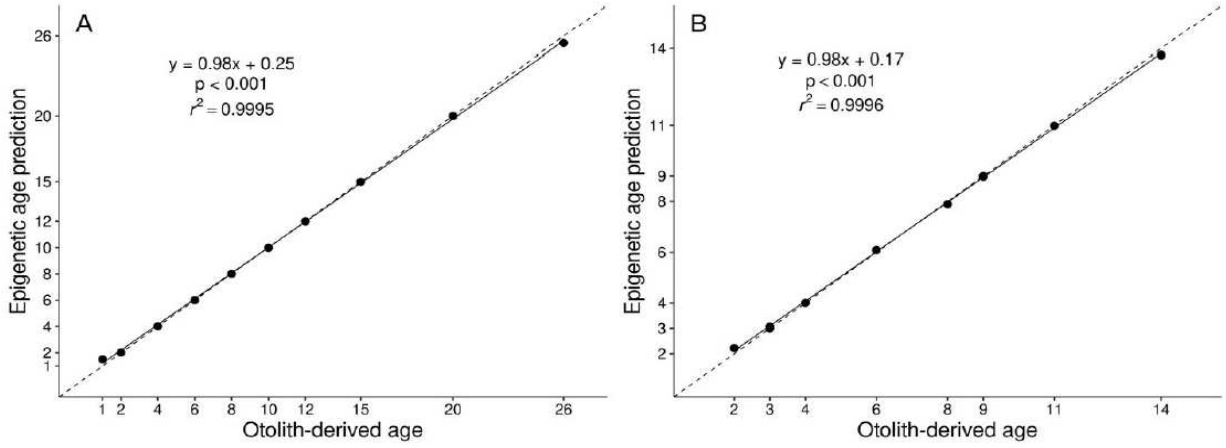

***Figure 16**: the epigenetic age predictions versus the otolith-derived ages for (A) the red snapper (the slope and the y intercept (± SE) are 0,98 (± 0,01) and 0,25 (± 0,09; r^2 = 0,9995)) and (B) the red grouper (the slope and the y intercept (± SE) are 0.98 (± 0,01) and 0,17 (± 0,05; r^2 = 0,9996)). The dashed lines indicate lines of 1:1 agreement between the predicted epigenetic and the otolith-derived ages. The solid lines represent linear regression that fits the data, with equations indicated on panels (Weber et al., 2022).*

For the first time, Weber et al. (2022) have determined epigenetic clocks for two species of wild reef fish without the use of zebrafish's biomarkers. Moreover, epigenetic clocks show a strong agreement between the predicted and otolith-derived ages despite the potential noise due to environmental heterogeneity (Weber et al. 2022). It has been demonstrated the possibility to collect and use diverse types of tissues, such as muscle and fin, both of which can be sampled non-lethally (Weber et al. 2022).

These revolutionary studies proved that epigenetic clocks can be widely applied for fisheries research, increasing the data diversity in stock assessments (Mayne et al., 2020; Mayne et al., 2020; Weber et al., 2022).

2. AIM OF THE THESIS

Considering the biological and economic importance of *Xiphias gladius*, the need for sustainable fishing practices, and the challenges associated with accurate age determination for this species, it is crucial to integrate novel age estimation methods for effective stock assessment. Based on these considerations, this thesis aimed to develop an epigenetic clock for *Xiphias gladius* based on 40 specimens from the southern Atlantic Ocean. Specifically, this research aims to identify CpG sites in the swordfish genome whose methylation levels correlate with aging, thereby facilitating the creation of a predictive model for estimating the species' age. Additionally, the thesis seeks to investigate the genomic regions that harbor these sites and the biological functions they perform. In doing so, the study will explore why these particular regions are associated with aging, shedding light on their role in the aging process.

3. METHODS AND MATERIALS

3.1 *Experimental design and sampling*

Forty samples of *Xiphias gladius* were caught in the Atlantic Ocean (Figure 17) from March 2018 to November 2018 and from March 2019 to November 2019, following guidelines established by ICCAT regarding commercial fishing.

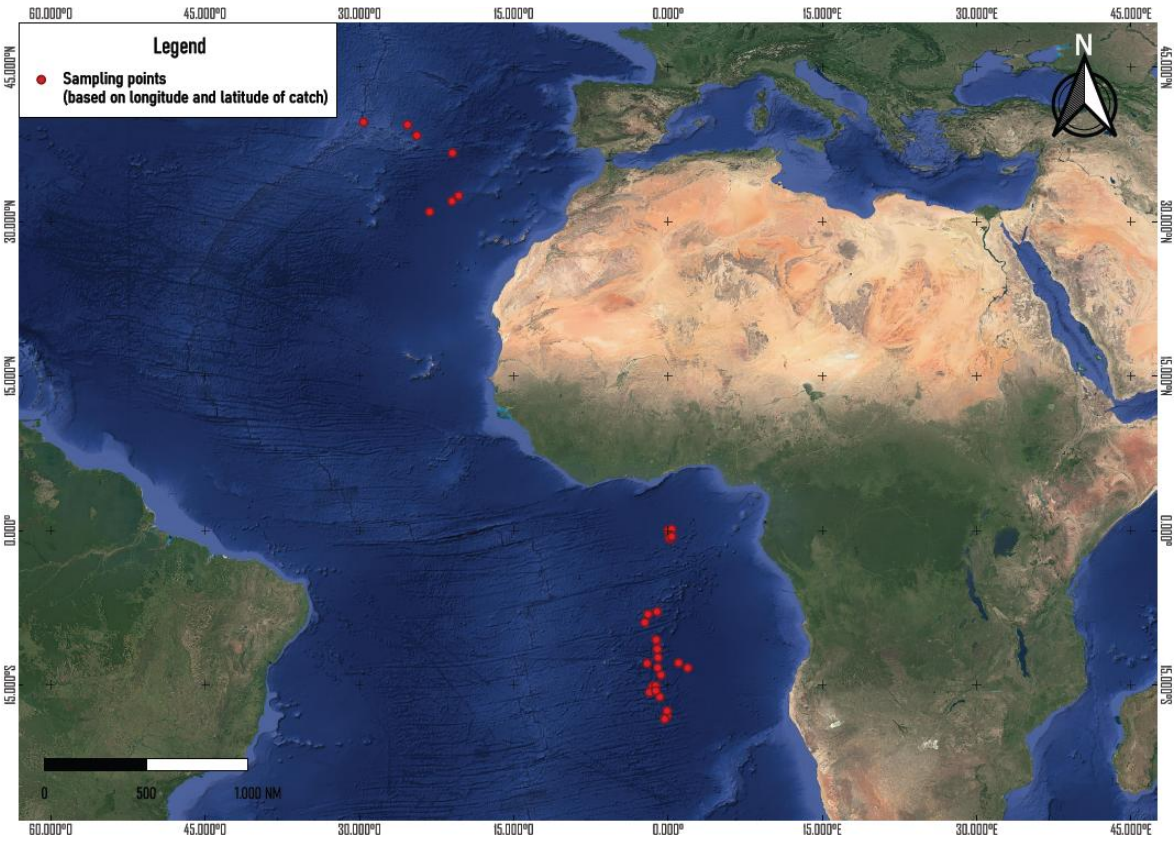

***Figure 17**: the sampling points, based on the longitude and latitude of the catch, are displayed on the map.*

During the sampling activities, the date and location of the catch, length, sex, maturity and stage of maturity of swordfish were collected (Table 1).

Sample_id	Caught_Lon	Caught_Lat	LJFL (cm)	Sex	Maturity	Maturity_stage
Xg3	-0,07	-17,99	222	F	Spent	Mature
Xg4	-2,25	-8,93	228	M	Spent	Mature
Xg26	-1,19	-15,6	133	M	Late_maturing	Mature
Xg34	0,25	-0,45	94	F	Immature	Immature
Xg35	0,25	-0,45	91	M	Immature	Immature
Xg36	0,36	-0,13	85	M	Immature	Immature
Xg37	-0,32	-18,32	168	M	Mature	Mature
Xg38	-0,07	-17,99	166	M	Late_maturing	Mature
Xg39	0,25	-0,45	78	F	Immature	Immature
Xg40	-0,32	-18,32	161	M	Mature	Mature
Xg42	0,36	-0,59	148	M	Late_maturing	Mature
Xg43	-0,8	-16,17	162	M	Late_maturing	Mature
Xg44	1,03	-12,87	172	M	Spent	Mature
Xg45	0,13	-0,73	141	M	Late_maturing	Mature
Xg48	-1,03	-11,53	226	F	Early_maturing	Mature
Xg50	36,68	-20,95	192	F	Late_maturing	Mature
Xg52	32,07	-21	148	F	Early_maturing	Mature
Xg53	39,43	-25,32	137	F	Early_maturing	Mature
Xg55	30,97	-23,16	93	M	Immature	Immature
Xg56	32,53	-20,35	108	F	Immature	Immature
Xg57	-1,2	-15,09	197	F	Mature	Mature
Xg58	-1,07	-7,89	228	F	Early_maturing	Mature
Xg59	-0,7	-14,03	151	M	Late_maturing	Mature
Xg60	-1,15	-10,63	146	F	Early_maturing	Mature
Xg61	-1,08	-10,92	193	M	Early_maturing	Mature
Xg63	-0,97	-12,35	173	F	Early_maturing	Mature
Xg65	-1,5	-15,13	211	F	Late_maturing	Mature
Xg66	-1,5	-15,13	146	M	Late_maturing	Mature
Xg67	-1,2	-15,09	197	F	Mature	Mature
Xg68	1,92	-13,36	145	M	Late_maturing	Mature
Xg69	-1,2	-15,09	182	F	Late_maturing	Mature
Xg73	-1,03	-11,53	170	F	Early_maturing	Mature
Xg74	39,68	-29,61	155	F	Immature	Immature
Xg75	-1	-13,34	192	F	Spent	Mature
Xg76	0,36	-0,59	148	M	Late_maturing	Mature
Xg77	-0,09	-17,53	207	M	Mature	Mature
Xg70	-2,03	-12,93	153	M	Late_maturing	Mature
Xg71	-1,19	-15,58	195	F	Mature	Mature
Xg54	38,38	-24,43	200	F	Early_maturing	Mature
Xg14	-1,94	-8,14	100	M	Immature	Immature

***Table 1**: data collected for the forty swordfish specimens analyzed.*

3.2 *DNA extraction*

After sampling, muscle samples were stored in ethanol at -20°C and transported to the "Laboratory of Developmental and Reproductive Biology" of "The

Polytechnic University of Marche" (Ancona, Italy). Here, samples were homogenized and digested through a lysis buffer (Tris-HCl, NaCl, EDTA, SDS and proteinase K) for DNA extraction purposes. This process was carried out using phenol and chloroform. The extracted DNA was purified through ethanol and sodium acetate washes. Quality and concentrations of the DNA were assessed respectively by electrophoresis and quantification with a spectrophotometer (IMPLEN, Nanophotometer NP80).

3.3 *Reduced Representation Bisulfite Sequencing* (*RRBS)*

Genomic DNA was subjected to RRBS library preparation using the Acegen Rapid RRBS Library Prep Kit (Acegen, Cat. No. AG0422) according to the manufacturer's protocol. In brief, 100 ng of genomic DNA was digested with MspI, end-repaired, 3'-dA-tailed and ligated to 5-methylcytosine-modified adapters. After bisulfite treatment, the DNA was amplified with 12 cycles of PCR using Illumina 8-bp dual index primers. Size selection was performed to obtain DNA fractions of MspI-digested products in the range of 100-350 bp using a dual-SPRI® protocol according to the manufacturer's protocol. The constructed RRBS libraries were then analyzed by Agilent 2100 Bioanalyzer and finally sequenced on Illumina platforms using a 150×2 paired-end sequencing protocol.

3.4 *Swordfish methylome characterization*

This section provides a detailed overview of the procedures conducted for the initial characterization of the methylome of swordfish (*Xiphias gladius*) using a Reduced Representation Bisulfite Sequencing (RRBS) approach.

The methodology spans several steps: Quality Control, Reference Generation, Bisulfite Mapping, Indexing and Extracting Methylation Ratios.

The primary objective of this workflow is to identify differentially methylated regions (DMRs) (also known as CpG islands) potentially associated with aging, thereby offering an initial epigenetic profile valuable for further research objectives. This technical section outlines each step, specifying the criteria, tools, and parameters employed to ensure transparency and reproducibility of the processes.

3.4.1 *Quality control*

To ensure high-quality data for downstream analyses, RRBS libraries were preprocessed using FastP (version 0.20.0). This step involved trimming reads to improve sequencing quality, while also generating a comprehensive Quality Control (QC) report for each sample. FastP is a tool designed for fast, all-in-one preprocessing of FASTQ files, which ensures that low-quality bases and adapter sequences are removed.

Additionally, FastQC (version 0.11.5) was used to produce clear, visual plots that allowed for easy comparison of quality scores between raw and trimmed samples.

For each sample and read direction, FASTQC analyses were performed both before and after trimming. This allowed to assess the quality of the raw sequencing data and evaluate the effectiveness of the trimming process.

3.4.2 *Reference generation*

The reference genome generation for bisulfite mapping in this project involved creating and indexing a formatted swordfish reference genome for efficient alignment. The specific reference genome file was prepared for indexing using bwa-meth index-mem2 (bwa-meth.py 0.2.7), optimizing it for memory-efficient read alignment and facilitating the accurate mapping of bisulfite-treated DNA sequences.

3.4.3 *Bisulfite Mapping*

For this section, bwa-meth (bwa-meth.py 0.2.7) is used for aligning bisulfite-treated DNA reads, which undergo cytosine-to-thymine conversions, making traditional alignment challenging. Bwa-meth is specifically optimized to handle these C-to-T mismatches, preserving methylation information during mapping.

Each sample's paired-end reads are aligned to the bisulfite-converted reference genome, sorted BAM files are generated in one step by piping the output to samtools sort (samtools 1.20), ensuring accurate, organized data for methylation analysis.

3.4.3.1 *Mapping Deduplication*

We conducted mapping deduplication using picard MarkDuplicates (picard 3.1.1) to optimize data quality for downstream methylation analysis. After bisulfite-treated DNA reads are aligned, deduplication becomes essential to remove biases introduced during library preparation and sequencing, specifically from duplicated reads that can artificially inflate methylation signals.

We utilize Picard's MarkDuplicates tool with specific parameters to remove sequencing duplicates (*REMOVE_SEQUENCING_DUPLICATES=true*), which primarily arise from library amplification and are unlikely to represent true biological signals while tagging only optical duplicates (*TAGGING_POLICY=OpticalOnly*), generated from sequencing artifacts, as they result from closely spaced clusters in the sequencing data that can mimic true reads. By retaining PCR duplicates, we allow downstream tools like MethylDackel to further evaluate and control for PCR-based artifacts, offering

a secondary filter to manage duplicates without prematurely discarding potential biological reads.

3.4.3.2 *Alignment QC*

To ensure the accuracy and reliability of our alignment and deduplication results, we performed alignment quality control (QC) using qualimap bamqc (qualimap 2.3.0). This step assesses the quality and characteristics of the mapped, deduplicated reads, providing metrics essential for interpreting alignment efficiency and coverage depth, which are crucial for downstream methylation analysis.

3.4.4 *Indexing*

To streamline downstream analyses, we prepared the reference genome and processed alignment files through several steps. First, BAM files from mapping and deduplication stages were indexed using samtools index to enable efficient random access during analysis. Additionally, the reference genome was indexed with samtools faidx (samtools 1.7), providing quick access to specific regions. To define consistent genomic intervals, we created a BED file using bedtools sort and bedtools merge (bedtools 2.30.0), which organizes overlapping intervals, enhancing computational efficiency for region-based analyses. Lastly, we generated bigWig files from the BAM files with bamCoverage (bamCoverage 3.4.3) to facilitate rapid visualization and

quantification of genomic coverage, essential for exploratory data inspection and downstream comparisons.

3.4.5 *Extracting Methylation Ratios*

MethylDackel extract (MethylDackel 0.6.1, using HTSlib version 1.20) was employed for extracting methylation ratios from bisulfite-converted and mapped BAM files. MethylDackel is specifically designed for bisulfite sequencing analysis, allowing for precise methylation calling across the genome. The *–keepDupes* argument is used to include all duplicate reads in the analysis, as optical duplicates were previously tagged but retained for methylation calling accuracy. This approach is valuable in bisulfite sequencing, where duplicate reads often carry crucial methylation information.

The workflow also leverages the previously indexed bigWig file with the *–mappability* argument, ensuring that low-mappability regions are accounted for when calculating methylation ratios. This integration helps reduce biases in repetitive or low-complexity regions, providing a more accurate representation of methylation levels across the genome.

3.5 *Methylation Analysis on Xiphias gladius*

Here, we started with the methylation calls from MethylDackel. Coverage was normalized with the median method. As described in Stubbs et al. (2017) we

first filtered CpG sites that had a mean coverage of < 2 reads, we applied an extra filter of > 130 reads (3rd. quartile of mean coverage) to remove spurious reads from library preparation and potential mapping artifacts. Furthermore, any site that was covered by < 5 reads in a particular sample was set to NA. Before calculating the mCpG-age association, sites were further filtered, forcing them to be covered in 90% of the samples (n = 612593).

To explore the correlation between methylation and length, we first used the cor.test function and the Pearson and Spearman methods to perform individual CpG correlations. P values were adjusted by the FDR method and CpGs with an adjusted p value of < 0.05 were considered length-correlated (similar to Bertucci et al., 2021). A MultiDimensional Scaling analysis (MDS) was performed using the stats dist function with the Euclidean method on the methylation percentage values of the significantly correlated CpGs to calculate the similarity matrix followed by the cmdscale function (k = 2 to represent 2D space).

To build the elastic net regression model, starting with the filtered set of CpGs (n = 612593), we first imputed missing values (~ 0.5 % of all measurements after the filtering) using 10-nearest-neighbor imputation using R package impute (Hastie et al., 2017). Finally, we split the dataset into a training and test set with 28 and 12 samples (70/30% split, which is broadly used), respectively.

The Length factor was natural log transformed and used as the response variable. The glmnet function was set to a 10-fold cross validation and an α-parameter of 0.5. The performance of the model was assessed using Pearson correlations, relative error rates and absolute error (Mayne et al., 2022).

Finally the ChIPseeker (Wang et al., 2022) R package was used to annotate the significantly correlated CpGs of the Pearson and Spearman correlations; and the elastic net regression model predictor CpGs. Furthermore, a Gene Ontology Enrichment Analysis (GOEA) and a Kyoto Encyclopedia of Genes and Genomes (KEGG) Enrichment Analysis were performed with the clusterProfiler package on the aforementioned sets of CpGs (padj < 0.05, BH method) while setting a minimum of 10 genes to perform the enrichment. Metabolic pathway visualizations for the significantly enriched KEGG terms were generated with pathview (Luo et al., 2013).

4. RESULTS

4.1 *Quality control, Bisulfite Mapping, Methylation analysis*

Before the RRBS libraries' construction, samples' quality was high for thirty-two samples (Quality Type A), moderate for two samples (Quality Type B), and low for six samples (Quality Type C). After the RRBS libraries' construction, the mean number of raw reads per sample was 78884864. Following Quality Control (QC), this decreased to 76990142 (97,6% of the initial read count) with 2,4% of low-quality or duplicated reads removed per sample. After the Mapping Deduplication, the mean number of mapped reads was 74236943, corresponding to 99,83% of the total reads (76990142), reflecting the alignment efficiency. On average, the methylation levels of 4660396 CpG sites were analyzed per sample, but after the last filtering, 612593 CpG sites remained for further analysis.

4.2 *Correlation between length and methylation status*

Method	Significant	Common_significant
Pearson	19051/612593 (3.11%)	15161/19051 (79.58%)
Spearman	19413/612593 (3.17%)	15161/19413 (78.1%)

Table 2: *the table shows summarized results of Pearson and Spearman correlation methods. The "Significant" column refers to the number of significant length-correlated CpGs in the 612593 filtered site for both methods. The "Common_significant" column refers to the number of CpGs identified as significant length-correlated by both methods.*

Considering Pearson's correlation, a total of 19051 significant length-correlated CpGs were identified out of the 612593 filtered CpG sites (Table 2). This represented 3,11% of the filtered sites. For Spearman's correlation, 19413 significant length-correlated CpGs were identified from the same 612593 filtered CpG sites, corresponding to 3,17% of the total filtered sites (Table 2). Of these significant length-correlated CpGs, 15161 common significant length-correlated CpGs were identified by both methods. These significant CpGs in common represented 79,58% and 78,1% of the significant CpGs identified using Pearson's and Spearman's method respectively (Table 2).

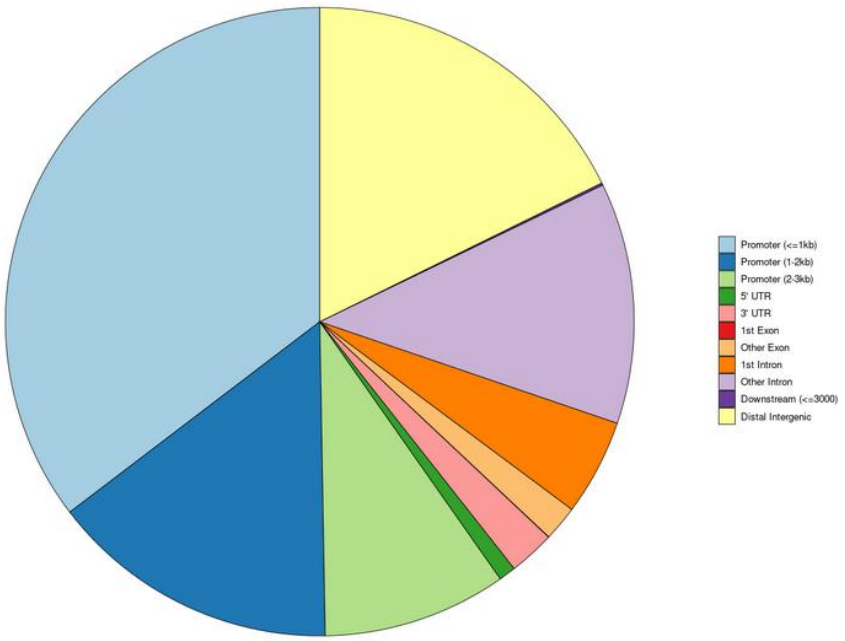

Figure 18: *pie chart of different genomic features of the significant length-correlated CpGs (for both Pearson's and Spearman's correlation). Each segment represents a different genomic feature, such as the promoter region, exons, introns, or untranslated regions (UTRs). The size of each segment indicates the percentage of significant CpGs associated with that feature.*

The 59,72% of significant length-correlated CpGs was located in promoters regions, specifically: 35,36% in promoters of ≤ 1 kb, 14,91% in promoters of 1-2 kb, and 9,45% in promoters of 2-3 kb (Figure 18).

Remaining sites were found in: distal intergenic (17,72%), other introns (12,40%), 1st intron (4,96%), 3' UTR (2,36%), other exons (1,82%), 5' UTR (0,87%), downstream (0,14%), 1st exon (0,01%) (Figure 18).

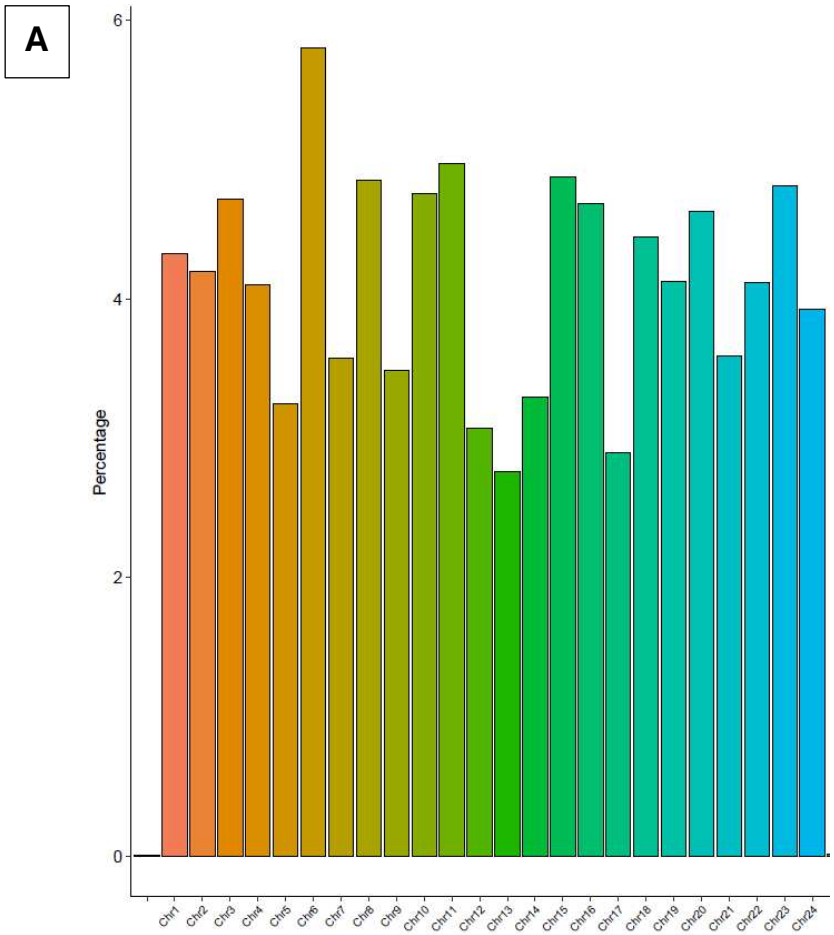

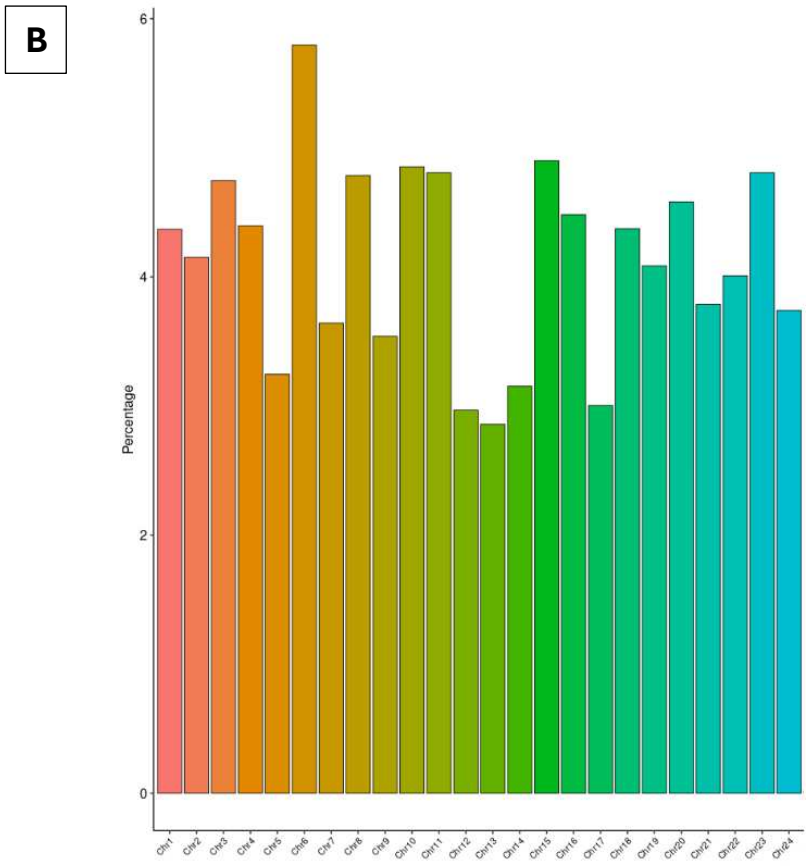

Figure 19: *distribution of the significant length-correlated CpGs for Pearson's (A) and Spearman's (B) correlation across the swordfish chromosomes. The X-axis displays chromosomes, the Y-axis shows the percentage of significant CpGs over chromosomes.*

Considering significant length-correlated CpGs for the Pearson's method (Figure 19 A), chromosome 6 hosted approximately 6% of the significant CpGs. To a lesser extent, chromosomes 1, 2, 3, 4, 8, 10, 11, 15, 16, 18, 19, 20, 22, and 23 each hosted between 4% and 5% of these sites. The remaining chromosomes contained less than 4% of these sites (Figure 19 A).

Considering length-correlated significant CpGs for the Spearman's method, chromosome 6 hosted approximately 6% of the significant CpGs. To a lesser

extent, chromosomes 1, 2, 3, 4, 8, 10, 11, 15, 16, 18, 19, 20, 22, and 23 each hosted between 4% and 5% of these sites. The remaining chromosomes contained less than 4% of these sites (Figure 19 B).

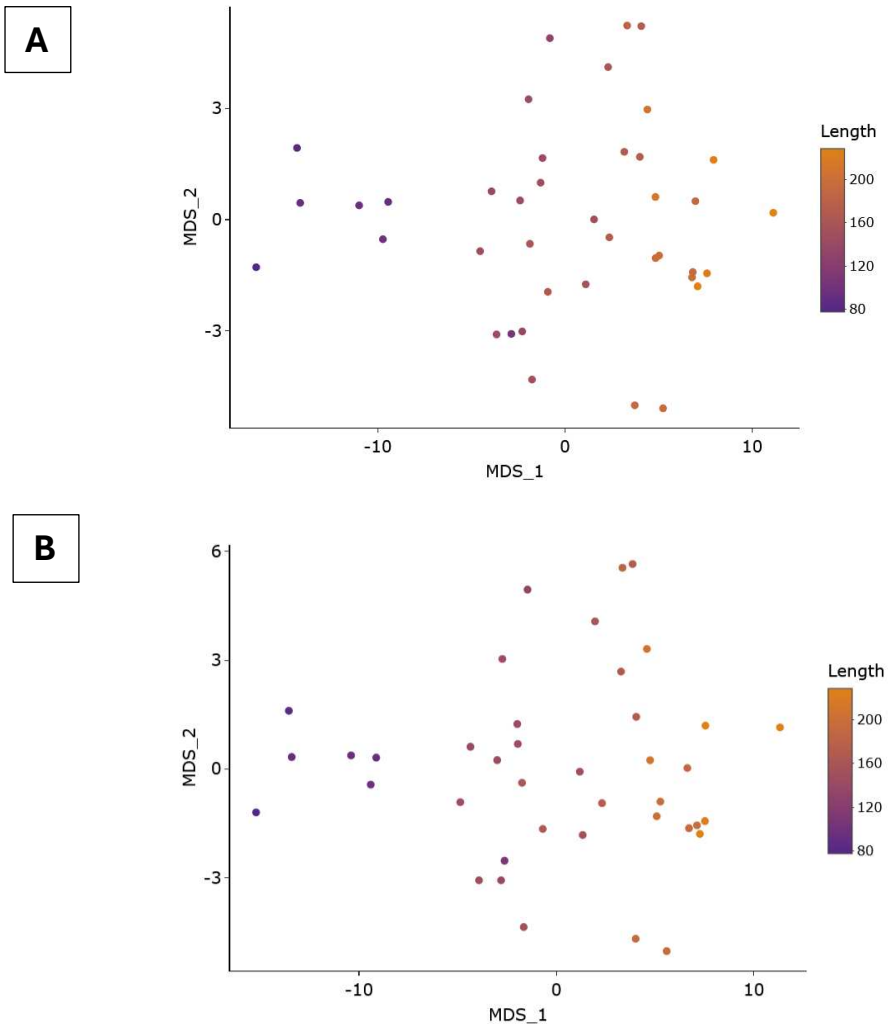

Figure 20: *MDS plots on the methylation percentage values of the significant length-correlated CpGs by Pearson (A) and Spearman (B). Each point corresponds to a sample, and the distances between points reflect the degree of similarity (or dissimilarity) in their methylation profiles. The color of the points ranges from blue to orange, with blue representing shorter individuals and orange representing the longest ones.*

In Figure 20, A and B, two distinct groups of samples were observed considering the MDS_1 axis. The first group, consisting of smaller individuals

(blue dots), was located to the left of the zero. The second group, composed of larger individuals (orange dots), was positioned to the right of zero of the same axis (Figure 20 A, B). For the first group of shorter individuals (blue dots), methylation levels of the significant length-correlated CpGs were different from those of larger individuals (orange dots) (Figure 20 A, B). No pattern emerged along the MDS_2 axis.

4.3 *Gene Ontology Enrichment Analysis of Correlating CpGs*

Gene Ontology enrichment analysis of 19051 length-correlated CpGs, evidenced 175 Biological Process significantly enriched (p adj<0.05). Noteworthy, most of them are related to head development, neurogenesis, ossification, cell fate commitment and endocrine system development (Figure 21).

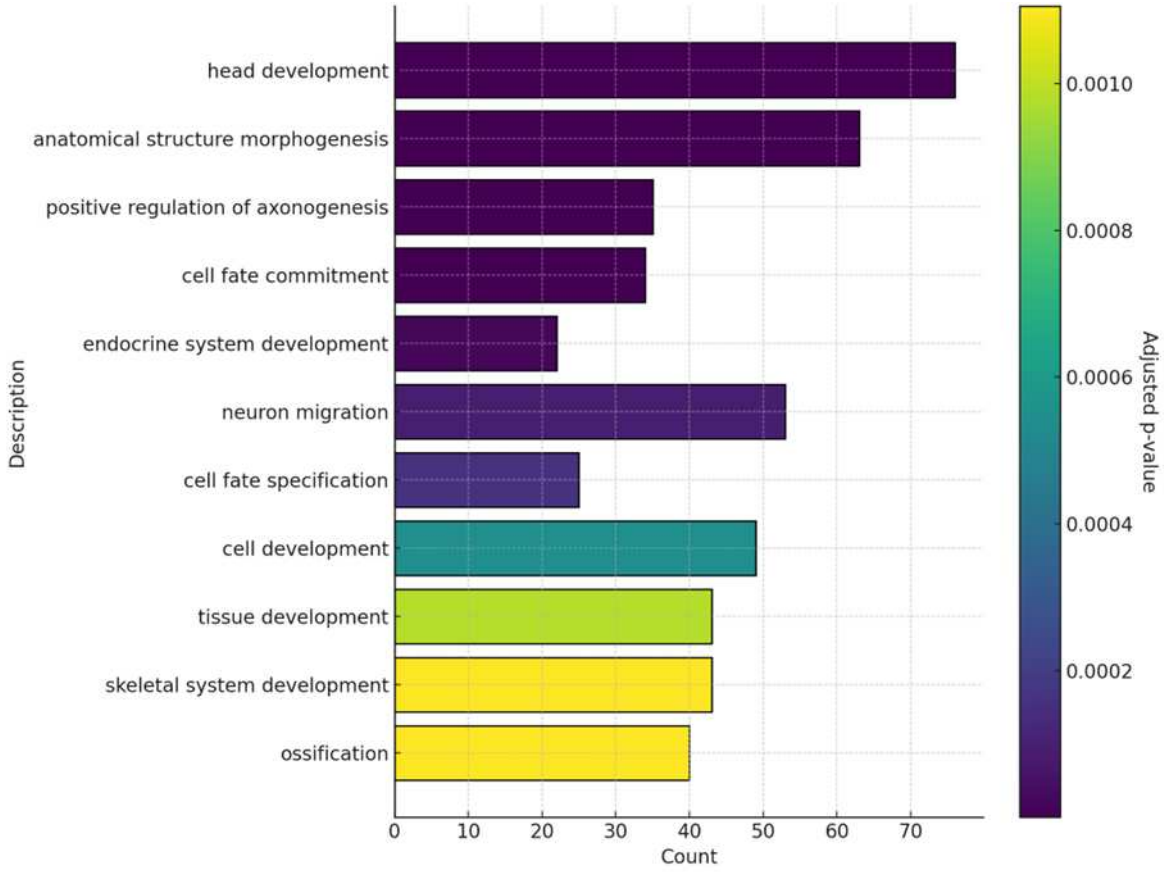

Figure 21: *the bar plot shows the results of the Gene Ontology Enrichment Analysis (GOEA) for the Correlating CpGs. The X-axis shows the count (number of genes annotated with the respective GO term). The Y-axis represents GO terms. The Adjusted p-value is used, and it is represented by colors, blue is used to indicate a high level of significance.*

4.4 *KEGG Enrichment Analysis of Correlating CpGs*

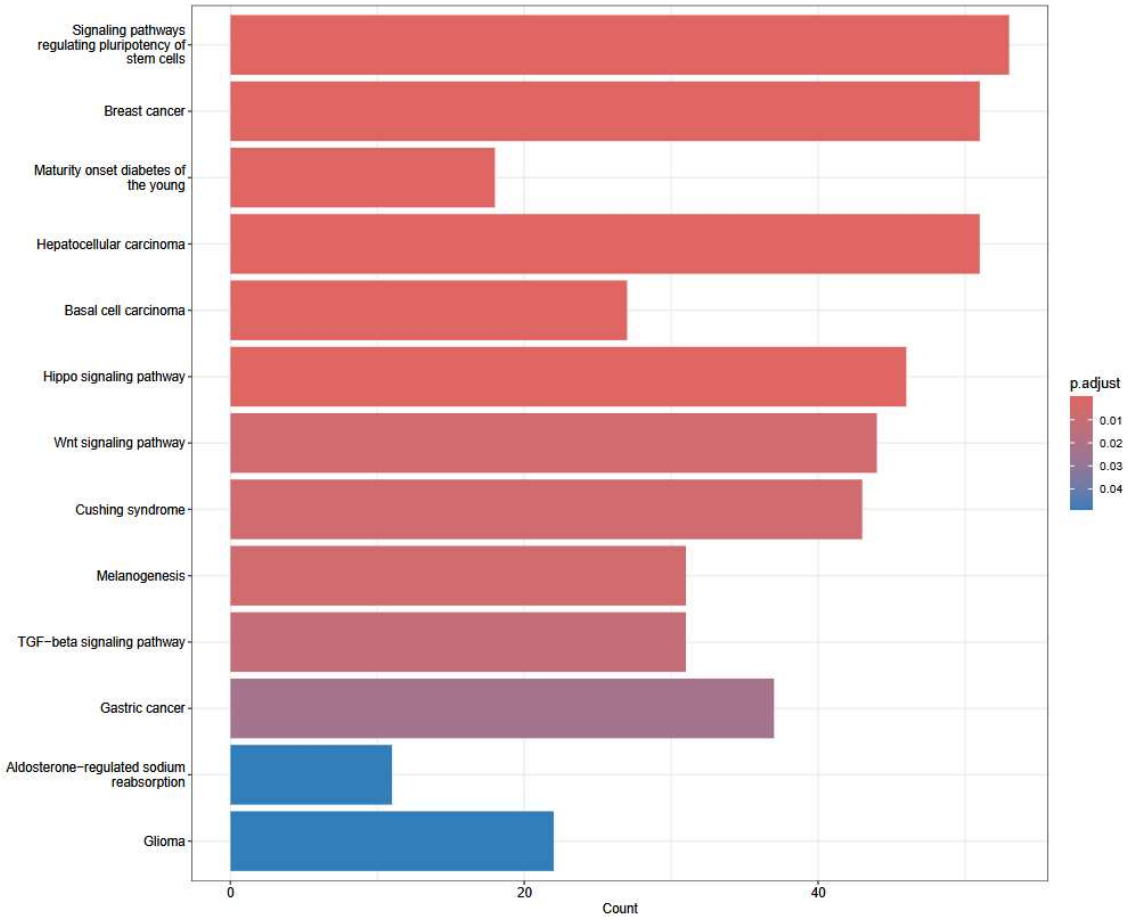

Figure 22: *bars plot shows the results of the Kyoto Encyclopedia of Genes and Genomes (KEGG) Enrichment Analysis for the Correlating CpGs. The X-axis shows the count (number of genes annotated with the respective pathway). The Y-axis represents the pathways in which the Correlating CpGs are involved. The adjust p-value (p.adjust) is used and it is represented by colors (red is the highest level of significance).*

Kyoto Encyclopedia of Genes and Genomes (KEGG) Enrichment Analysis of 19051 length-correlated CpGs, evidenced 13 pathways significantly enriched (p adj < 0.05). Noteworthy, most of them are related to carcinogenesis (Figure 22 and 23).

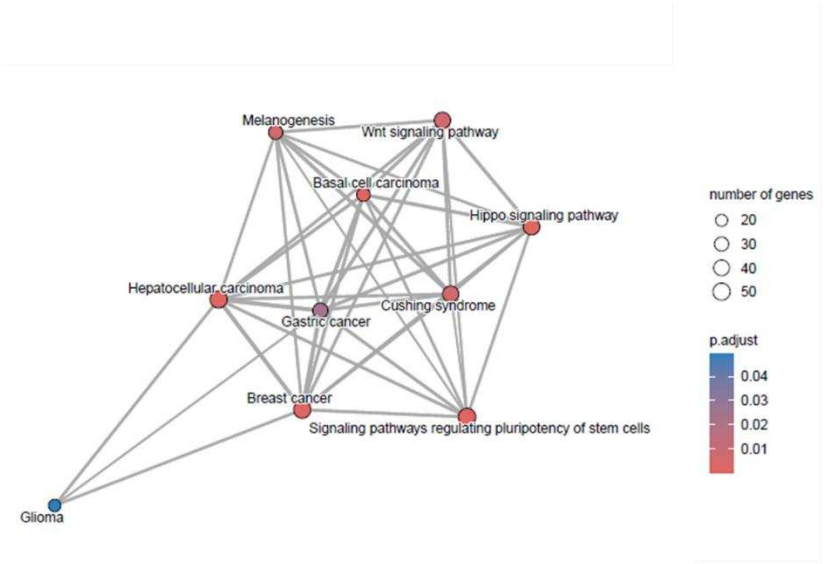

Figure 23: *Emap plot of enriched "kegg pathways". p.adjust = the Benjamini–Hochberg adjusted P-value for the enriched kegg pathways. Size = the number of genes which belong to the enriched kegg pathways.*

4.5 *Elastic net regression model*

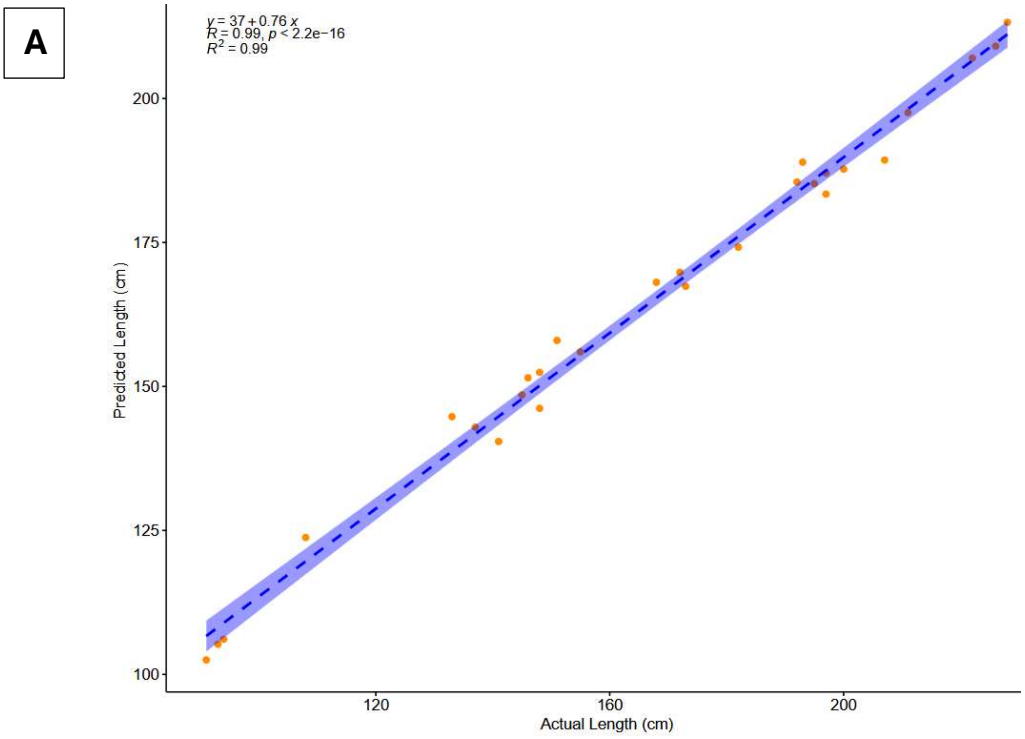

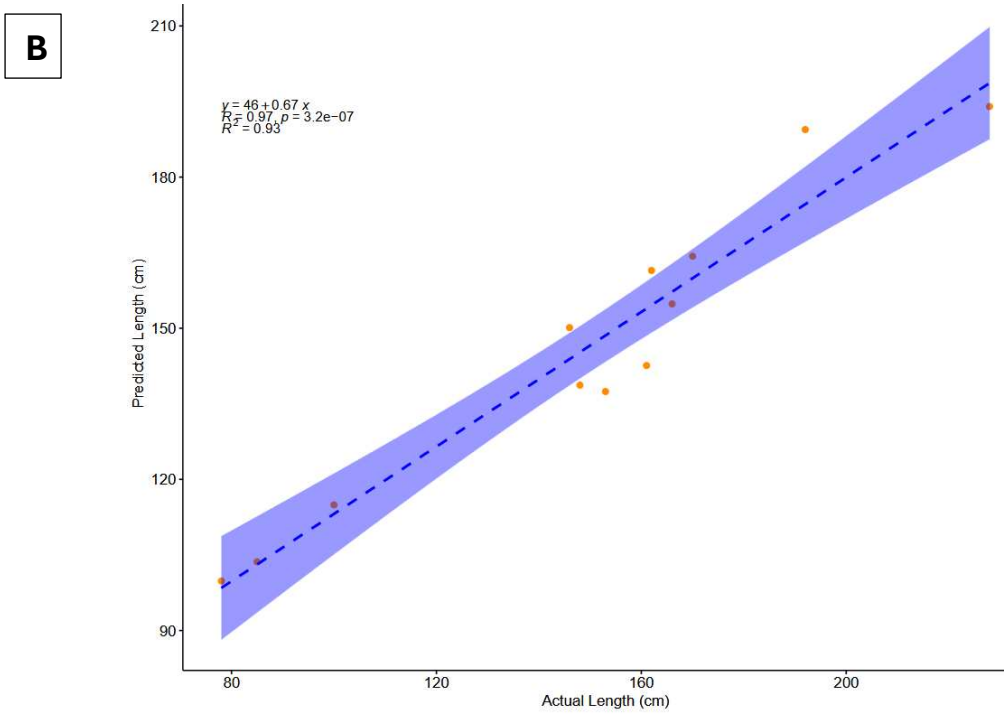

Figure 24: *performance of the elastic net regression model in training (A) and testing (B) data set. The X-axis represents the actual length (known length). The Y-axis represents the predicted length (from methylation level). Each point represents a sample. A blue dashed regression line illustrates the linear relationship between the predicted and actual values, along with the associated confidence interval. The Pearson's correlation coefficient (R) and the equation of the regression line are displayed on each plot.*

The elastic net regression model identified 57 optimal CpG sites required for predicting length (annotated to forty-eight unique genes). Using these 57 CpG sites, it was observed a strong correlation between the actual and predicted lengths in both the training (Pearson's correlation = 0,99, p-value < $2{,}20 \times 10^{-16}$) and testing (Pearson's correlation = 0,97, p-value = $3{,}20 \times 10^{-7}$) datasets (Figure 24).

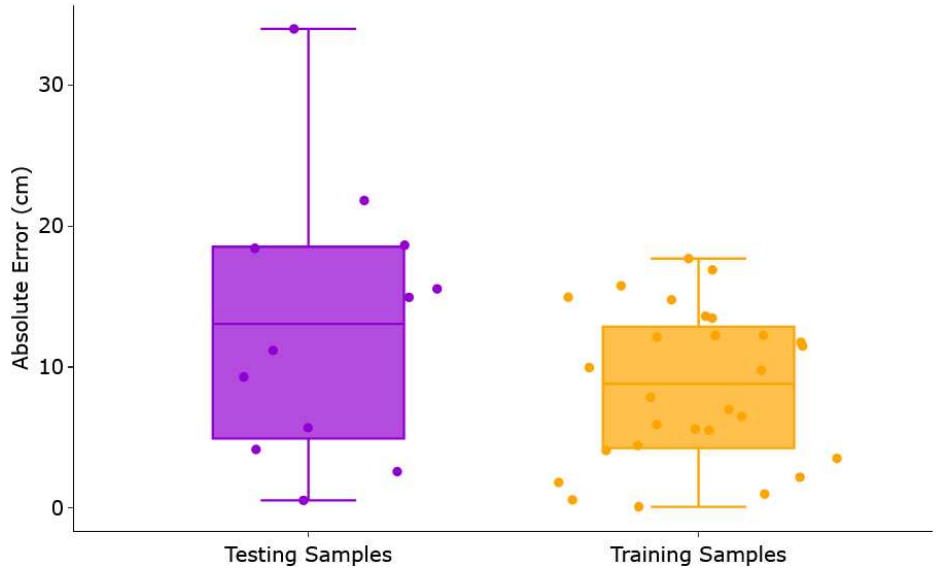

Figure 25: *boxplot shows the median absolute error rate (MAE) in the training (right) and testing (left) data sets. The X-axis represents the dataset (either Training Samples or Testing Samples). The Y-axis shows the absolute error between the predicted and actual values. Points represent the single samples and are used for aesthetic purposes only.*

The median absolute error rate (MAE) was 13 cm and 9 cm for the testing and training datasets respectively (Figure 25), corresponding to a relative error of 5,73% when comparing the testing MAE to the maximum length in the testing dataset. The absolute error was not statistically different between the two datasets (two-tailed t test, p value = 0,156), indicating the robustness and good performance of the model.

4.6 *Predictor CpGs*

This set of 57 CpGs was the one used for the model to predict the swordfish length, therefore called Predictor CpGs.

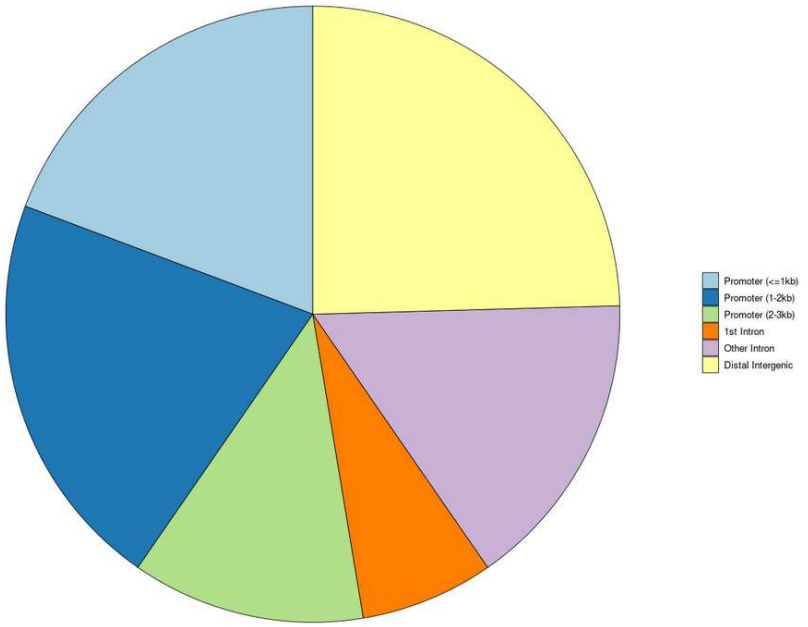

Figure 26: pie *chart of different genomic features for Predictor CpGs. Each segment represents a different genomic feature, such as promoters or introns. The size of each segment indicates the percentage of Predictor CpGs associated with that feature.*

The 52,63% of the Predictor CpGs was located in promoter regions, specifically: 19,30% in promoters of ≤ 1 kb, 21,05% in promoters of 1-2 kb, and 12,28% in promoters of 2-3 kb (Figure 26). The remaining sites were found in: distal intergenic (24,6%), other introns (15,79%), and 1st intron (7,02%) (Figure 26).

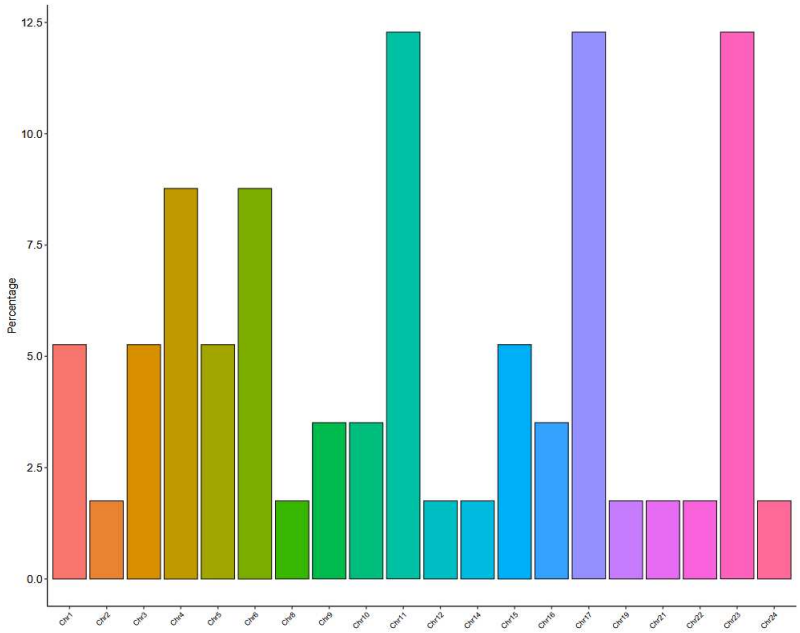

Figure 27: *Predictor CpGs distribution across swordfish chromosomes. The X-axis displays the chromosomes. The Y-axis shows the percentage of Predictor CpGs in each chromosome.*

Chromosomes 11, 17, and 23 hosted 12,5% of Predictor CpGs. Chromosomes 4 and 6 hosted between 7,5% and 10% of these sites. To a lesser extent, chromosomes 1, 3, 5, and 15 hosted 5% of these sites. The remaining chromosomes contained less than 5% of these sites (Figure 27).

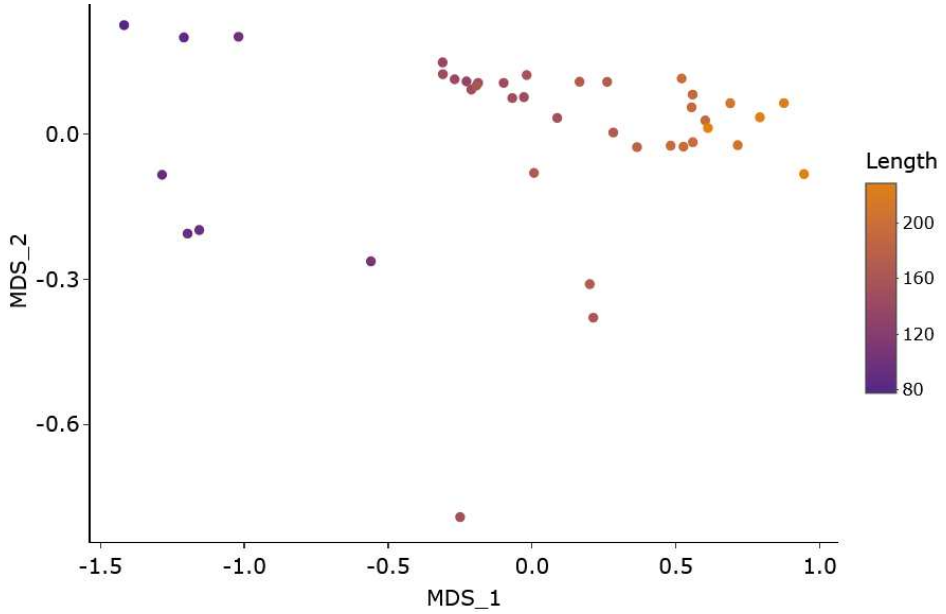

Figure 28: *the MDS plots produced with the Predictor CpGs methylation level. Each point corresponds to a sample, and the distances between points reflect the degree of similarity (or dissimilarity) in their methylation profiles. The color of the points ranges from blue to orange, with blue representing the shorter individuals and orange representing the larger ones.*

Two main groups of samples emerged with two distinct clusters within the data (Figure 28). The first group, consisting of shorter individuals (blue dots), was found between -1.0 and -1.5 on the MDS_1 axis, while the second group, composed of larger individuals (orange dots), was found between -0.5 and 1 on the same axis.

For the first group of shorter individuals (blue dots), the methylation levels of the Predictor CpGs were different from those of larger individuals (orange dots) (Figure 28).

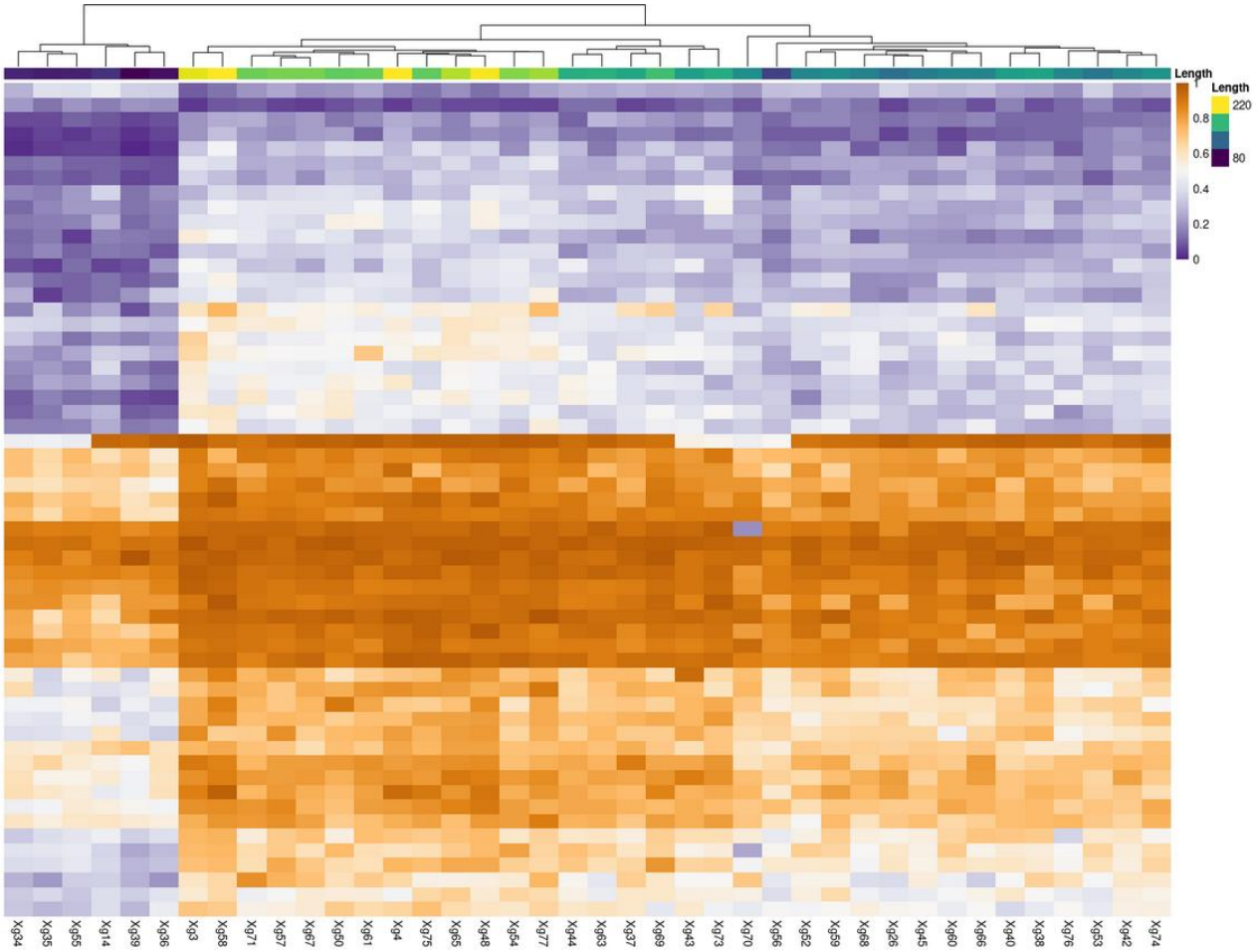

Figure 29: *heatmap plot of the methylation percentage values of the Predictor CpGs. In the upper part of the graph, the hierarchical clustering of the samples is shown. Each branch leads to a small rectangle representing an individual sample. The color of the rectangle, which corresponds to the sample, can be blue, light blue, green, or yellow, depending on the sample's length. Each column represents a sample, and the sample name is displayed at the bottom of each column. Each row represents a CpG site. The color of the rows reflects the methylation percentage of the corresponding CpG site.*

Two main hierarchical clusters were observed, the largest one was further divided into three smaller subclusters (Figure 29).

The first main cluster consisted of six specimens (from Xg34 to Xg36) characterized by small lengths (blue samples), and it was positioned on the top-left side of the graph (Figure 29).

The second main cluster included 34 specimens (from Xg3 to Xg74) of varying lengths (samples ranging from light blue to yellow). This cluster could be further subdivided into three smaller clusters based on hierarchical clustering: 1st subcluster (Xg3 to Xg77), 2nd subcluster (Xg44 to Xg73), 3rdsubcluster (Xg70 to Xg74) (Figure 29).

Distinct methylation patterns were observed between these clusters, based on the methylation percentages of the Predictor CpGs. A key difference was seen between the first and second main clusters in terms of methylation levels. Specifically, the first main cluster (Xg34 to Xg36) exhibited much lower methylation levels across the Predictor CpGs compared to the second main cluster (Xg3 to Xg74) (Figure 29).

The methylation profile for the first main cluster was as follows: between 0% and 20% in the first 24 CpG sites; between 50% and 100% for CpG sites 25 to 40; between 40% and 60% for CpG sites 40 to 57 (Figure 29).

In contrast, the second main cluster showed: methylation between 0% and 60% for the first 24 CpG sites, between 70% to 100% for CpG sites 25 to 40 and between 40% and 100% for CpG sites 40 to 57 (Figure 29).

Interestingly, the methylation pattern of the Predictor CpGs in the first main cluster closely resembled that of 3rd subcluster (Xg70 to Xg74). However, the

first main cluster still maintained distinct differences in methylation percentages compared to 1st subcluster (Xg3 to Xg77) and 2nd subcluster (Xg44 to Xg73).

5. DISCUSSION

Managing an unhealthy stock in an overexploited area affected by overfishing, urgently requires accurate and sustainable methods to assess the status of commercially important species. Developing these methods is crucial to ensuring the long-term viability of the stock (ICCAT, 2023). Indeed, one of the key challenges in managing fish populations is the reliable determination of age, as traditional methods, such as otolith, vertebrae and fin-ray analysis, can be time-consuming, invasive, and often yield inaccurate results (Campana, 2001; Millot et al., 2024), especially for species like *Xiphias gladius*. For this reason, forty *Xiphias gladius* specimens were selected from the South Atlantic stock in order to develop an epigenetic clock that could provide a more efficient alternative for age estimation, with potential implications for better conservation and stock management for a stock that is still little known (ICCAT, 2023).

To ensure a robust and representative model, swordfish specimens were carefully selected, including twenty males and twenty females at various stages of sexual maturity, ranging from small, young individuals to large, older ones. This approach included a broad spectrum of biological variability, which is essential for avoiding bias and developing a universally applicable model.

For the DNA extraction, the choice of tissue type was made in favour of muscle, as previously done by Anastasiadi & Piferrer (2020).

At this point, it was essential to determine the most appropriate sequencing technique to guarantee the success of the study. In fact, the RRBS method was chosen to develop the swordfish epigenetic clock, owing to its advantages over other sequencing techniques (Beck et al., 2022). This choice was supported by successful results obtained in studies by Mayne et al. (2022) and Weber et al. (2022), both of which employed RRBS for the same purpose on green turtle and reef fishes, respectively. In addition to its well-known advantages, RRBS proved particularly effective in this study. It enabled the analysis of low-quality samples, despite 20% of the swordfish samples having degraded DNA (Quality Type B and C). These samples were collected six to seven years ago, and the RRBS method demonstrated its robustness in handling lower-quality DNA.

The fact that the RRBS technique was highly effective in sequencing was also confirmed by bioinformatics analyses. These analyses included quality control steps to remove contaminants and duplicates from the RRBS sequencing results to improved data reliability. Although a considerable proportion of the raw reads was expected to be discarded due to the low-quality of the initial DNA samples, only 2,4% was filtered out during quality control. This result further highlighted the efficiency of the RRBS, which guarantees the processing of a

vast number of reads, with over seventy-five million (76990142) successfully retained. Continuing with the bioinformatics analysis, additional filtering steps were applied to remove spurious reads from library preparation and potential mapping artifacts. These steps ensured that only the most informative reads were retained for downstream analysis. At the end of these processes, the number of CpG sites identified from the total reads amounted to 612593. These sites were the focus of the methylation analysis related to length.

Compared to studies conducted to date, the number of CpG sites initially investigated in this study is exceptionally high (612593), especially when compared to the 21369 CpGs (but from 8000 samples) identified by Horvat (2013), 37 CpGs by Polanowski et al. (2014), 2338 CpGs by De Paoli-Iseppi et al. (2019), and 48 CpGs by Anastasiadi & Piferrer (2020). The authors approaching the number of CpGs initially investigated in this study were: Thompson et al. (2018) which selected an initial dataset of 193651 CpGs, Mayne et al. (2022) which selected 1261168 CpGs, and Weber et al. (2022) which selected 49189 CpG sites. As shown in this and the studies of Thompson et al. (2018), Mayne et al. (2022), Weber et al. (2022), by coincidence RRBS has proven to be the optimal method for investigating methylation levels across a large number of CpG sites.

At this point, we were ready to explore the potential correlation between CpG site methylation levels and the age of our samples. Unfortunately, due to the unavailable data on the age of the 40 individuals used in the analysis, the epigenetic clock was developed based on the available data, more specifically on length data (LFLJ). This variable was chosen because grow rates by age for the South Atlantic swordfish stock are well documented (Garcia et al., 2017), allowing for an indirect estimation of age (Campana and Thorrold, 2001). Once age data for the selected individuals becomes available, an age-calibrated epigenetic clock will be developed. This would allow for more precise age estimations in the future.

To develop the epigenetic clock, it was essential to determine whether any of the 612593 initial CpGs were significantly correlated with the samples' length. Based on this, over 19000 length-correlated sites were identified using two different statistical methods (19051 for Pearson and 19413 for Spearman).

To gain insight in the processes that contribute to epigenetic clock progression, we adopted a functional genomics approach in which we systematically evaluated the association between CpGs related to length and genome-wide gene expression as read-out of the biological changes involved in progression of aging. An initial analysis of these sites revealed a predominant presence on chromosome 6 (Figure 19) and within promoter regions of the genome (Figure

18), suggesting their involvement in regulation of the gene expression. However, one of the most striking findings emerged from the MDS represented in Figure 20. This graph clearly demonstrated that shorter individuals (younger ones) exhibited a gradual change in methylation levels as they grew longer, corresponding to older individuals. These results, along with other observed correlations, underscored the clear relationship between the methylation levels of the length-correlated CpGs and swordfish length.

To gain a deeper understanding of this relationship, two additional analyses were performed: Gene Ontology Enrichment Analysis (GOEA) and KEGG pathway analysis. The GOEA revealed that most length-correlated CpG sites were located within genes involved in biological processes related to development and organismal growth. Specifically, many of the genes associated with these sites were involved in head development, skeletal tissue formation, tissue and cell development, endocrine system development, ossification, neuron migration, and the positive regulation of axogenesis (Figure 21). In parallel, KEGG pathway analysis highlighted the involvement of a large number of length-correlated CpG sites in molecular pathways associated with carcinogenesis, including glioma, melanogenesis, gastric cancer, and hepatocellular carcinoma (Figures 22 and 23).

These findings demonstrate that the genes associated with the 19051 CpGs not only regulate processes driving individual growth, such as length increase, but also contribute to organismal deterioration, ultimately leading to death. Although these processes and pathways may seem opposite, they share a common link to aging. In fact, while developmental processes are active in younger individuals, they gradually decline with age (Kishi et al., 2004; Boskey & Coleman, 2010; Bergmans et al., 2023). As this occurs, alternative pathways, including those linked to carcinogenesis, may become more pronounced (Anisimov et al., 2009).

Moreover, their expression appeared to be regulated by methylation, which is influenced by environmental factors, including time (Jung & Pfeifer, 2015). Indeed, the methylation levels of CpG sites on these genes change over time during the growth, with consequences for gene expression (Jung & Pfeifer, 2015). As a result, a young organism could exhibit a methylation profile at length-correlated CpG sites that supports the expression of genes involved in development, such as head development. As the individual reaches its maximum length, which corresponds to a specific age (Garcia et al., 2019), the methylation levels of these CpG sites could begin to repress developmental pathways and activate carcinogenesis-related pathways, such as glioma, ultimately contributing to the individual's death.

Once discovered and deeply analyzed the relationship between the methylation levels of the 19051 CpG sites and swordfish's length, it was reasonable to hypothesize that some of these CpGs might be strongly associated with the fish length, to the point of being able to predict an individual's length starting from the methylation levels of few length-correlated CpGs.

Building on this hypothesis, 57 CpG sites were selected from the elastic net regression model to predict the swordfish length (Figure 24), yielding an accuracy of 0,97 (R^2 = 0,97; p-value = $3{,}20 \times 10^{-7}$) and a precision of 13 cm (which measures the average difference between the predicted and observed lengths in the tested samples) (Figure 25). Although the model was trained with only 28 samples and tested with 12 (total of 40 individuals), it produced highly accurate results, particularly when compared to studies conducted to date. In fact, the accuracy of the swordfish epigenetic clock was exceptionally high compared to the 0,79 accuracy of the clock developed by Polanowski et al. (2014) using 63 individuals with 3 final CpGs per sample, the 0,59 accuracy reported by De Paoli-Iseppi et al. (2019) with 71 individuals and 7 final CpGs per sample, the 0,79 to 0,89 accuracy obtained by Thompson et al. (2018) using 1189 individuals with 952 final CpGs per sample, and the 0,82 accuracy from Anastasiadi & Piferrer (2020) with 50 individuals and 16 final CpGs per sample. The authors whose accuracy approached that of the swordfish

epigenetic clock include Mayne et al. (2022), with an accuracy of 0,90 using 63 individuals and 29 final CpGs per sample, and Weber et al. (2022), with an accuracy of 0,99 using 10 individuals and 199 final CpGs per sample.

Thanks to this result, it will now be possible to predict the swordfish's length based on the methylation levels of few CpG sites, and indirectly estimate its age (Garcia et al., 2017). Furthermore, as the machine learning model continues to be trained, it will not only improve the accuracy of length predictions but also reduce the number of CpG sites involved in the prediction process.

As already observed for the nineteen thousand length-correlated sites, the 57 CpG sites were also located in promoter regions of the genome (Figure 26), although their distribution across chromosomes differs (Figure 27). Both the MDS results in Figure 28 and the heatmap in Figure 29 confirm what was previously observed in the MDS for the length-correlated CpGs (Figure 20). One novel finding that emerged from the heatmap was the clear distinction in methylation patterns of the 57 CpG sites between the group of six immature individuals (first large cluster) (Figure 29) and the group of thirty-four mature individuals (second large cluster) (Figure 29). This marked difference suggests that it may be possible to discriminate sexual maturity in this species based on methylation levels. This discovery could revolutionize studies on sexual maturity in swordfish and pave the way for innovative approaches in scientific

research, especially in underexplored areas like the South Atlantic. Moreover, it could set a precedent for similar studies on this, and other commercially significant species threatened by overfishing.

6. CONCLUSION

This study opens new possibilities in the stock management of commercially and biologically significant fish species, such as *Xiphias gladius*. Initially, the epigenetic approach was viewed as a tool for validating age obtained with traditional methods (otoliths, vertebrae, fin-ray analysis). However, recent evidences, supported by this study, suggest that epigenetics could play a pivotal role in direct and indirect age determination. Through the analysis of genome methylation levels, a DNA sample could provide valuable insights into an individual's length, age, as well as its sexual maturity. Information that were once difficult to obtain, costly, time-consuming, and prone to loss or inaccuracy can now be gathered with a single, highly efficient test. Such advancements could mark the beginning of a new era, where epigenetics becomes the primary method to determine all types of data in future stock assessments, also leading to a deeper and more comprehensive understanding of marine life.

REFERENCES

Abascal, F. J., Mejuto, J., Quintans, M., & Ramos-Cartelle, A. (2010). Horizontal and vertical movements of swordfish in the Southeast Pacific. *ICES Journal of Marine Science*, *67*(3), 466-474. doi: https://doi.org/10.1093/icesjms/fsp252.

Abascal, F. J., Mejuto, J., Quintans, M., García-Cortés, B., & Ramos-Cartelle, A. (2015). Tracking of the broadbill swordfish, *Xiphias gladius*, in the central and eastern North Atlantic. *Fisheries Research*, *162*, 20-28. doi: http://dx.doi.org/10.1016/j.fishres.2014.09.011 0165-7836.

Abid N., Laglaouri A., Arakrak A., Bakkali M. (2016). Preliminary results on sex ratio and maturity of the swordfish (*Xiphias gladius*) in the strait of Gibraltar; implications for the stocks structure. Collect. Vol. Sci. Pap. ICCAT, 72(8): 2042-2050.

Abid N., Laglaoui A., Arakrak A. Bakkali M. (2018). The reproductive biology of swordfish (*Xiphias gladius*) in the Strait of Gibraltar. *J. Mar. Biol. Assoc. United Kingdom* 1–11. doi: https://doi.org/10.1017/S0025315418000346.

Abid, N., Laglaoui, A., Arakrak, A., & Bakkali, M. (2019). The reproductive biology of swordfish (*Xiphias gladius*) in the Strait of Gibraltar. *Journal of the Marine Biological Association of the United Kingdom*, 99(3), 649-659. doi:10.1017/S0025315418000346.

Akyol, O., & Ceyhan, T. (2013). Age and growth of swordfish (*Xiphias gladius* L.) in the Aegean Sea. *Turkish Journal of Zoology*, 37(1), 59-64. doi: 10.3906/zoo-1204-3.

Alıçlı, T. Z., Oray, I. K., Karakulak, F. S., & Kahraman, A. E. (2012). Age, sex ratio, length-weight relationships and reproductive biology of Mediterranean swordfish, *Xiphias gladius* L., 1758, in the eastern Mediterranean. *African Journal of Biotechnology*, *11*(15), 3673-3680. doi: 10.5897/AJB11.2189.

Anastasiadi, Dafni, and Francesc Piferrer (2020). "A clockwork fish: Age prediction using DNA methylation-based biomarkers in the European seabass." *Molecular Ecology Resources* 20.2: 387-397. doi: https://doi.org/10.1111/1755-0998.13111.

Anisimov, V. N., Sikora, E., & Pawelec, G. (2009). Relationships between cancer and aging: a multilevel approach. *Biogerontology*, *10*, 323-338. doi: https://doi.org/10.1007/s10522-008-9209-8.

Beck, Daniel, Millissia Ben Maamar, and Michael K. Skinner (2022). "Genome-wide CpG density and DNA methylation analysis method (MeDIP, RRBS, and WGBS) comparisons." *Epigenetics* 17.5: 518-530. doi: https://doi.org/10.1080/15592294.2021.1924970.

Behjati, Sam, and Patrick S. Tarpey (2013). "What is next generation sequencing?." *Archives of Disease in Childhood-Education and Practice* 98.6: 236-238. doi:10.1136/archdischild-2013-304340.

Bergmans, S., Raes, L., Moons, L., & De Groef, L. (2023). A review on neurodegeneration in the fast-ageing killifish, the first animal model to study the natural occurrence of neuronal cell loss. *Ageing Research Reviews*, 102065. doi: https://doi.org/10.1016/j.arr.2023.102065.

Bertucci, E. M., Mason, M. W., Rhodes, O. E., & Parrott, B. B. (2021). Exposure to ionizing radiation disrupts normal epigenetic aging in Japanese medaka. *Aging (Albany NY)*, *13*(19), 22752. doi: https://doi.org/10.18632/aging.203624.

Boskey, A. L., & Coleman, R. (2010). Aging and bone. *Journal of dental research*, *89*(12), 1333-1348. doi: 10.1177/0022034510377791.

Braun, C. D., Gaube, P., Afonso, P., Fontes, J., Skomal, G. B., Thorrold, S. R., and Kaplan, D. (2019). Assimilating electronic tagging, oceanographic modelling, and fisheries data to estimate movements and connectivity of swordfish in the North Atlantic. *ICES Journal of Marine Science*, *76*(7), 2305–2317. doi: https://doi.org/10.1093/icesjms/fsz106.

Bremer, J. A., Mejuto, J., Gómez-Márquez, J., Pla-Zanuy, C., Viñas, J., Marques, C., ... & Greig10, T. W. (2007). Genetic population structure of Atlantic swordfish: current status and future directions. *Collective Volume of Scientific Papers,* ICCAT, 61, 107-118.

Brock, H.W., Fisher, C.L. (2005). Maintenance of gene expression patterns. *Developmental Dynamics* 232, 633–655. doi: 10.1002/dvdy.20298.

Campana, Steven E. (1997): "Use of radiocarbon from nuclear fallout as a dated marker in the otoliths of haddock *Melanogrammus aeglefinus*." *Marine Ecology Progress Series* 150: 49-56. doi:10.3354/meps150049**.**

Campana, Steven E. (1999): "Chemistry and composition of fish otoliths: pathways, mechanisms and applications." *Marine ecology progress series* 188: 263-297. doi:10.3354/meps188263

Campana, S. E. (2001). Accuracy, precision and quality control in age determination, including a review of the use and abuse of age validation methods. *Journal of fish biology*, *59*(2), 197-242. doi: https://doi.org/10.1111/j.1095-8649.2001.tb00127.x.

Campana, S. E., & Thorrold, S. R. (2001). Otoliths, increments, and elements: keys to a comprehensive understanding of fish populations?. *Canadian Journal of Fisheries and Aquatic Sciences*, *58*(1), 30-38. Doi: https://doi.org/10.1139/f00-177.

Cavalieri V, Spinelli G. (2017): Environmental epigenetics in zebrafish. *Epigenetics Chromatin*. doi: https://doi.org/10.1186/s13072-017-0154-0 PMID:28982377.

Casselman, J. M. (1983). Age and growth assessment of fish from their calcified structures—techniques and tools. *NOAA Technical Report NMFS*, *8*, 1-17.

Chatterjee, A., Rodger, E. J., Morison, I. M., Eccles, M. R., & Stockwell, P. A. (2017). Tools and strategies for analysis of genome-wide and gene-specific DNA methylation patterns. *Oral biology: molecular techniques and applications*, 249-277. doi: 10.1007/978-1-4939-6685-1_15.

Choat, J. H., & Robertson, D. R. (2002). Age-based studies. *Coral reef fishes: dynamics and diversity in a complex ecosystem*, 57-80.

Collette, B. B., McDowell, J. R., & Graves, J. E. (2006). Phylogeny of recent billfishes (Xiphioidei). *Bulletin of Marine Science*, *79*(3), 455-468.

Corriero A., Acone, F., Desantis, S., Zubani, D., Deflorio M., Ventriglia G., Bridges C.R., Labate M., Palmieri G., McAllister B. G., Kime D. E., De Metrio G. (2004). Histological and immunohistochemical investigation on ovarian development and plasma estradiol levels in the swordfish (*Xiphias gladius* L.). *European Journal of Histochemistry*, vol. 48 issue 4:413-422. doi: https://doi.org/10.4081/915.

Deans, C., Maggert, K. A. (2015). What do you mean, "Epigenetic"? *Genetics* 199, 887–896. doi: 10.1534/genetics.114.173492.

DeMartini, E. E., Uchiyama, J. H., Humphreys, R. L., Sampaga, J. D., & Williams, H. A. (2007). Age and growth of swordfish (*Xiphias gladius*) caught by the Hawaii-based pelagic longline fishery. *Fishery Bulletin*, 105, 356‑367.

De Paoli-Iseppi, R., Deagle, B. E., Polanowski, A. M., McMahon, C. R., Dickinson, J. L., Hindell, M. A., & Jarman, S. N. (2019). Age estimation in a long-lived seabird (*Ardenna tenuirostris*) using DNA methylation-based biomarkers. *Molecular ecology resources*, *19*(2), 411-425. doi: https://doi.org/10.1111/1755-0998.12981.

Ehrhardt, N. M., Robbins, R. J., & Arocha, F. (1996). Age validation and growth of swordfish, *Xiphias gladius*, in the Northwest Atlantic. *Collective Volume of Scientific Papers*, ICCAT, 45, 358‑367.

Erauskin-Extramiana, M., Arrizabalaga, H., Cabre, A., Coelho, R., Rosa, D., Ibaibarriaga, L., & Chust, G. (2020). Are shifts in species distribution triggered by climate change? A swordfish case study. *Deep Sea Research Part II: Topical Studies in Oceanography*, *175*, 104666. doi: https://doi.org/10.1016/j.dsr2.2019.104666.

Esteves, E., Simões, P., Silva, H. M., & Andrade, J. P. (1995). Ageing of swordfish, *Xiphias gladius* Linnaeus, 1758, from the Azores, using sagittae, anal-fin spines and vertebrae. *ARQUIPÉLAGO. Ciências Biológicas e Marinhas= Life and Marine Sciences*, *13*, 39-51. doi: http://hdl.handle.net/10400.3/2108.

Farley, J. H., Clear, N. P., Krusic-Golub, K., Eveson, J. P., & Young, J. W. (2022). A bone to pick with age estimation using hard parts: A case study of swordfish, *Xiphias gladius*, in the Southwest Pacific Ocean. *Fisheries*. doi: https://doi.org/10.1016/j.fishres.2022.106413.

Fritsches, K. A., Brill, R. W., & Warrant, E. J. (2005). Warm eyes provide superior vision in swordfishes. *Current Biology*, *15*(1), 55-58.

Garcia, A., Tserpes, G., & Santos, M. N. (2017). Validation of annulus formation and growth estimation of South Atlantic swordfish. *Journal of the Marine Biological Association of the United Kingdom*, *97*(7), 1511-1518. doi: https://doi.org/10.1017/S0025315416000862.

Garma, L. D., & Quintela-Fandino, M. (2024). Applicability of epigenetic age models to next-generation methylation arrays. *Genome medicine*, *16*(1), 116. doi: https://doi.org/10.1186/s13073-024-01387-4.

Gerhard, G. S. (2003). Comparative aspects of zebrafish (*Danio rerio*) as a model for aging research. *Experimental Gerontology*, *38*(11-12), 1333-1341. doi: https://doi.org/10.1016/j.exger.2003.10.022 PMID:14698814.

Ghemrawi, M., Tejero, N. F., Duncan, G., & McCord, B. (2023). Pyrosequencing: Current forensic methodology and future applications—A review. *Electrophoresis*, *44*(1-2), 298-312. doi: https://doi.org/10.1002/elps.202200177.

Gilbert, M. J., Zerulla, T. C., & Tierney, K. B. (2014). Zebrafish (*Danio rerio*) as a model for the study of aging and exercise: Physical ability and trainability decrease with age. *Experimental gerontology*, *50*, 106-113. doi: https://doi.org/10.1016/j.exger.2013.11.013 PMID:24316042.

Gioacchini, G., Pappalardo, L., Pignalosa, P., & Carnevali, O. (2019). Females reproductive biology of Mediterranean swordfish (*Xiphias gladius* L.)*:* New insights from a multidisciplinary study. SCRS/2019/027, ICCAT.

Gu, H., Smith, Z. D., Bock, C., Boyle, P., Gnirke, A., & Meissner, A. (2011). Preparation of reduced representation bisulfite sequencing libraries for genome-scale DNA methylation profiling. *Nature protocols*, *6*(4), 468-481. doi: https://doi.org/10.1038/nprot.2010.190.

Guo, W., Fiziev, P., Yan, W., Cokus, S., Sun, X., Zhang, M. Q., ... & Pellegrini, M. (2013). BS-Seeker2: a versatile aligning pipeline for bisulfite sequencing data. *BMC genomics*, *14*, 1-8. doi: https://doi.org/10.1186/1471-2164-14-774.

Habegger, M. L., Dean, M. N., Dunlop, J. W., Mullins, G., Stokes, M., Huber, D. R., ... & Motta, P. J. (2015). Feeding in billfishes: inferring the role of the rostrum from a biomechanical standpoint. *The Journal of Experimental Biology*, *218*(6), 824-836. doi: https://doi.org/10.1242/jeb.106146.

Hastie, T. J. (2017). Generalized additive models. In *Statistical models in S* (pp. 249-307). Routledge.

Hazin F.H.V., Hazin, H.G., Boeckmann, C.E., and Travassos, P. (2002). Preliminary study on the reproductive biology of swordfish, *Xiphias gladius* (Linnaeus 1758), in the southwestern equatorial Atlantic ocean. *Col. Vol. Sci. Pap.* ICCAT, 54(5): 1560-1569.

Heimbrand, Y., Limburg, K. E., Hüssy, K., Casini, M., Sjöberg, R., Palmén Bratt, A. M., Levinsky, S. E., Karpushevskaia, A., Radtke, K., & Öhlund, J. (2020). Seeking the true time: Exploring otolith chemistry as an age-determination tool. *Journal of Fish Biology*, 97(2), 552‐565. doi: https://doi.org/10.1111/jfb.14422.

Heyn, H., Li, N., Ferreira, H. J., Moran, S., Pisano, D. G., Gomez, A., ... & Esteller, M. (2012). Distinct DNA methylomes of newborns and centenarians. *Proceedings of the National Academy of Sciences*, *109*(26), 10522-10527. doi: 10.1073/pnas.1120658109.

Hermann, A., Gowher, H., & Jeltsch, A. (2004). Biochemistry and biology of mammalian DNA methyltransferases. *Cellular and Molecular Life Sciences CMLS*, *61*, 2571-2587. doi: https://doi.org/10.1007/s00018-004-4201-1.

Horvath, S. (2013). DNA methylation age of human tissues and cell types. *Genome Biology*, 14(10), R115. Retrieved from http://genomebiology.com/2013/14/10/R115/. doi: https://doi.org/10.1186/gb-2013-14-10-r115.

Hüssy, K., Krüger-Johnsen, M., Thomsen, T. B., Heredia, B. D., Næraa, T., Limburg, K. E., ... & Radtke, K. (2021). It's elemental, my dear Watson: validating seasonal patterns in otolith chemical chronologies. *Canadian Journal of Fisheries and Aquatic Sciences*, *78*(5), 551-566. doi: https://doi.org/10.1139/cjfas-2020-0388.

ICCAT, 2023. Report for Biennial Period, 2022-23, Part II, Vol. 2.

Integrated Taxonomic Information System (ITIS). (2008). Istiophoridae ITIS Taxonomic Serial No.: 172486. Retrieved December 27, 2008.

Jelinek, J., & Madzo, J. (2016). DREAM: a simple method for DNA methylation profiling by high-throughput sequencing. *Chronic myeloid leukemia: methods and protocols*, 111-127. doi: https://doi.org/10.1007/978-1-4939-4011-0_10.

Jung, M., & Pfeifer, G. P. (2015). Aging and DNA methylation. *BMC Biology*, 13, 7. doi: 10.1186/s12915-015-0118-4.

Kalish, J. M., Johnston, J. M., Gunn, J. S., & Clear, N. P. (1996). Use of the bomb radiocarbon chronometer to determine age of southern bluefin tuna *Thunnus maccoyii*. *Marine Ecology Progress* Series, 143, 1‑8. doi: https://doi.org/10.3354/meps143001.

Kalish, J. M. (2002). *Use of the bomb radiocarbon chronometer to validate fish age*. Fisheries Research and Development Corporation [and] Australian National University.

Kasapidis, P., Valeiras, X., García-Cortés, B., & Mejuto, J. (2008). Genetic and growth profiles of several specimens of swordfish (*Xiphias gladius*) tagged and recaptured in the Atlantic, Indian and Pacific oceans. ICCAT *Coll Vol Sci Pap*, *62*(4), 1142-51.

Keller JM, Keller ET. (2018). The use of mature zebrafish (*Danio rerio*) as a model for human aging and disease. *Conn's Handbook of Models for Human Aging: Elsevier*, pp. 351–59. doi: https://doi.org/10.1016/B978-0-12-811353-0.00026-9.

Kishi S. (2004). Functional aging and gradual senescence in zebrafish. *Annals of the New York Academy of Sciences*, *1019*(1), 521-526. doi: https://doi.org/10.1196/annals.1297.097 PMID:15247079.

Lerner, J. D., Kerstetter, D. W., Prince, E. D., Talaue-McManus, L., Orbesen, E. S., Mariano, A., ... & Thomas, G. L. (2013). Swordfish vertical distribution and habitat use in relation to diel and lunar cycles in the western North Atlantic. *Transactions of the American Fisheries Society*, *142*(1), 95-104. doi: https://doi.org/10.1080/00028487.2012.720629.

Logan, J. M., Golet, W., Smith, S. C., Neilson, J., & Van Guelpen, L. (2021). Broadbill swordfish (*Xiphias gladius*) foraging and vertical movements in the north-west A tlantic. *Journal of Fish Biology*, *99*(2), 557-568. doi: https://doi.org/10.1111/jfb.14744.

Lowerre-Barbieri, S. K., Ganias, K., Saborido-Rey, F., Murua, H., & Hunter, J. R. (2011). Reproductive timing in marine fishes: variability, temporal scales, and methods. *Marine and Coastal Fisheries*, *3*(1), 71-91. doi: https://doi.org/10.1080/19425120.2011.556932.

Lu, A. T., Fei, Z., Haghani, A., Robeck, T. R., Zoller, J. A., Li, C. Z., ... & Singh, K. (2021). Universal DNA methylation age across mammalian tissues. *BioRxiv*, 2021-01. doi: 10.1038/s43587-023-00462-6.

Luo, W., & Brouwer, C. (2013). Pathview: an R/Bioconductor package for pathway-based data integration and visualization. *Bioinformatics*, *29*(14), 1830-1831. doi: https://doi.org/10.1093/bioinformatics/btt285.

Macías, D., Hattour, A., De Serna, J. M., & Godoy, D. (2005). Reproductive characteristics of swordfish (*Xiphias gladius*) caught in the southwestern Mediterranean Sea during 2003. *Collective Volume of Scientific Papers* ICCAT, 58, 454–469.

Mamoozadeh, N. R., Graves, J. E., Bealey, R., Schratwieser, J., Holdsworth, J. C., Ortega-Garcia, S., & McDowell, J. R. (2023). Genomic data resolve long-standing uncertainty by distinguishing white marlin (*Kajikia albida*) and striped marlin (*K. audax*) as separate species. *ICES Journal of Marine Science*, *80*(6), 1802-1813. doi: https://doi.org/10.1093/icesjms/fsad114.

Marisaldi, L. (2021). La biologia riproduttiva del pesce spada *Xiphias gladius* e del tonno rosso atlantico thunnus thynnus nel mar Mediterraneo: basi per una gestione sostenibile della pesca. doi: https://hdl.handle.net/11566/290113.

Mayne, B., Korbie, D., Kenchington, L., Ezzy, B., Berry, O., & Jarman, S. (2020). A DNA methylation age predictor for zebrafish. *Aging (Albany NY)*, *12*(24), 24817. doi: 10.18632/aging.202400.

Mayne, B., Farley, J., Feutry, P., Bravington, M., & Davies, C. (2020). Rapid epigenetic age estimation for southern bluefin tuna. In *Prepared for the Extended Scientific Committee for the Twenty Fifth Meeting of the Scientific Committee*.

Mayne, B., Mustin, W., Baboolal, V., Casella, F., Ballorain, K., Barret, M., ... & Berry, O. (2022). Age prediction of green turtles with an epigenetic clock. *Molecular Ecology Resources*, *22*(6), 2275-2284. doi: https://doi.org/10.1111/1755-0998.13621.

Metzker, M. L. (2010). Sequencing technologies—the next generation. *Nature reviews genetics*, *11*(1), 31-46. doi: https://doi.org/10.1038/nrg2626.

Mhanni, A. A., & McGowan, R. A. (2004). Global changes in genomic methylation levels during early development of the zebrafish embryo. *Development of genes and evolution*, *214*, 412-417. https://doi.org/10.1007/s00427-004-0418-0 PMID:15309635.

Millot, R., Vanalderweireldt, L., Finelli Sandolo, L., & Durieux, E. D. (2024). Age estimates derived from hard parts of swordfish *Xiphias gladius* from the north-western Mediterranean Sea. *Journal of Fish Biology*, *104*(1), 56-68. doi: https://doi.org/10.1111/jfb.15558.

Nakamura, I. (1985). *FAO species catalogue. Vol. 5. Billfishes of the world. An annotated and illustrated catalogue of marlins, sailfishes, spearfishes and swordfishes known to date* (No. 125, pp. iv+-65pp).

Nishimoto, R. N., DeMartini, E. E., & Landgraf, K. C. (2006). Suitability of sagittae for estimating annular ages of swordfish, *Xiphias gladius*, from the central North Pacific.

National Institute of Water and Atmospheric Research (NIWA) (2012). Determining the age of fish. Retrieved from https://niwa.co.nz/fisheries/research-projects/determining-the-age-of-fish.

Palko, B. J., Beardsley, G. L., & Richards, W. J. (1981). *Synopsis of the biology of the swordfish, Xiphias gladius Linnaeus* (No. 127). US Department of Commerce, National Oceanic and Atmospheric Administration, National Marine Fisheries Service.

Piferrer, F., & Anastasiadi, D. (2022). State of the Art Review of age prediction in fishes using epigenetic clocks. doi: http://hdl.handle.net/10261/297265.

Piferrer, F., & Anastasiadi, D. (2023). Age estimation in fishes using epigenetic clocks: Applications to fisheries management and conservation biology. *Frontiers in Marine Science*, *10*, 1062151. doi: https://doi.org/10.3389/fmars.2023.1062151.

Pine, W. E., Pollock, K. H., Hightower, J. E., Kwak, T. J., & Rice, J. A. (2003). A review of tagging methods for estimating fish population size and components of mortality. *Fisheries*, *28*(10), 10-23. doi: https://doi.org/10.1577/1548-8446(2003)28[10:AROTMF]2.0.CO;2.

Poisson, F., & Fauvel, C. (2009). Reproductive dynamics of swordfish (*Xiphias gladius*) in the southwestern Indian Ocean (Reunion Island). Part 1: oocyte development, sexual maturity and spawning. *Aquatic Living Resources*, *22*(1), 45-58. doi:10.1051/alr/2009007.

Polanowski, A. M., Robbins, J., Chandler, D., & Jarman, S. N. (2014). Epigenetic estimation of age in humpback whales. *Molecular ecology resources*, *14*(5), 976-987. doi: https://doi.org/10.1111/1755-0998.12247.

Prince, E. D., Lee, D. W., & Berkeley, S. A. (1988). Use of marginal increment analysis to validate the anal spine method for ageing Atlantic swordfish and other alternatives for age determination. *ICCAT Coll. Vol. Sci. Pap*, *27*, 194-201.

Quelle, P., González-Blázquez, F., Ruiz, M., Valeiras, J., Gutiérrez-Martín, L. Ó., Rodriguez-Marin, E., & Mejuto-García, J. (2014). An approach to age and growth of South Atlantic swordfish (*Xiphias gladius*) stock. *Centro Oceanográfico de A Coruña*. doi: http://hdl.handle.net/10261/322438.

Rafferty, S. A., & Quinn, T. A. (2018). A beginner's guide to understanding and implementing the genetic modification of zebrafish. *Progress in biophysics and molecular biology*, *138*, 3-19. doi: https://doi.org/10.1016/j.pbiomolbio.2018.07.005 PMID:30032905.

Righi, T., Splendiani, A., Fioravanti, T., Petetta, A., Candelma, M., Gioacchini, G., ... & Barucchi, V. C. (2020). Mediterranean swordfish (*Xiphias gladius* Linnaeus, 1758) population structure revealed by microsatellite DNA: genetic diversity masked by population mixing in shared areas. *PeerJ*, *8*, e9518. doi: 10.7717/peerj.9518.

Romeo, T., Consoli, P., Greco, S., Canese, S., & Andaloro, F. (2009). Swordfish (*Xiphias gladius*, Teleostea: Xiphiidae) surface behaviour during reproductive period in the central Mediterranean Sea (southern Tyrrhenian Sea). *Marine Biodiversity Records*, *2*, e45. doi:10.1017/S1755267209000578.

Ronaghi, M. (2001). Pyrosequencing sheds light on DNA sequencing. *Genome research*, *11*(1), 3-11. doi:10.1101/gr.150601.

Rosa, D., Garibaldi, F., Snodgrass, D., Orbesen, E., Santos, C., Macías-López, Á. D., ... & Coelho, R. (2022). Update on the satellite tagging of atlantic and mediterranean swordfish. *Centro Oceanográfico de Málaga*. doi: http://hdl.handle.net/10261/325962.

Saber, S., de Urbina, J. O., Gillespie, K., Poisson, F., Coelho, R., Rosa, D., ... & Macías, D. (2020). A preliminary analysis of the maturity of ICCAT swordfish stocks. *Collect. Vol. Sci. Pap. ICCAT*, *77*(3), 537-551.

Smith, B. L., Lu, C. P., García-Cortés, B., Viñas, J., Yeh, S. Y., & Alvarado Bremer, J. R. (2015). Multilocus Bayesian estimates of intra-oceanic genetic differentiation, connectivity, and admixture in Atlantic swordfish (*Xiphias gladius* L.). *PLoS One*, *10*(6), e0127979. doi: https://doi.org/10.1371/journal.pone.0127979.

Stears, R. L., Martinsky, T., & Schena, M. (2003). Trends in microarray analysis. *Nature medicine*, *9*(1), 140-145. doi: https://doi.org/10.1038/nm0103-140.

Stoehr, A., St. Martin, J., Aalbers, S., Sepulveda, C., & Bernal, D. (2018). Free-swimming swordfish, *Xiphias gladius*, alter the rate of whole body heat transfer: morphological and physiological specializations for thermoregulation. *ICES Journal of Marine Science*, *75*(2), 858-870. doi: https://doi.org/10.1093/icesjms/fsx163.

Stubbs, T. M., Bonder, M. J., Stark, A. K., Krueger, F., von Meyenn, F., Stegle, O., & Reik, W. (2017). Multi-tissue DNA methylation age predictor in mouse. *Genome biology*, *18*, 1-14. doi: https://doi.org/10.1186/s13059-017-1203-5.

Sun, C. L., Wang, S. P., & Yeh, S. Z. (2002). Age and growth of the swordfish (*Xiphias gladius* L.) in the waters around Taiwan determined from anal-fin rays. *Fishery Bulletin*, 100, 822‑835.

Surya, S., Rohit, P., Abdussamad, E. M., Landge, A., Santhosh, B., Nayak, B. B. & Anil, M. K. (2022). Taxonomy of BIllfishes. URI: http://eprints.cmfri.org.in/id/eprint/15715.

Takahashi, M., Okamura, H., Yokawa, K., and Okazaki, M. (2003). Swimming behaviour and migration of a swordfish recorded by an archival tag. *Marine and Freshwater Research*, *54*(4), 527–534. doi: https://doi.org/10.1071/MF01245.

Thompson, M. J., Chwiałkowska, K., Rubbi, L., Lusis, A. J., Davis, R. C., Srivastava, A., ... & Pellegrini, M. (2018). A multi-tissue full lifespan epigenetic clock for mice. *Aging (Albany NY)*, *10*(10), 2832. doi: doi: 10.18632/aging.101590.

Trucchi, E., Mazzarella, A.B., Gilfillan, G.D., Lorenzo, M.T., and Schönswetter, O.P. (2016). BsRADseq: screening DNA methylation in natural populations of non-model species. 323 *Mol. Ecol*. doi:10.1111/mec.13550.

Tserpes, G., & Tsimenides, N. (1995). Determination of age and growth of swordfish, *Xiphias gladius* L, 1758, in the eastern Mediterranean using anal-fin spines. *Fishery Bulletin*, 93, 594‑602.

Uchiyama, J. H., Skillman, R. A., Sampaga, J. D., & DeMartini, E. E. (1998). A preliminary assessment of the use of hard parts to age central Pacific swordfish, *Xiphias gladius*. *NOAA Tech. Rep. NMFS*, *142*, 261-273.

Videler, J. J., Haydar, D., Snoek, R., Hoving, H.-J. T., & Szabo, B. G. (2016). Lubricating the swordfish head. *Journal of Experimental Biology*, 219(13), 1953-1956. doi: https://doi.org/10.1242/jeb.139634.

Wang, Q., Li, M., Wu, T., Zhan, L., Li, L., Chen, M., ... & Yu, G. (2022). Exploring epigenomic datasets by ChIPseeker. *Current Protocols*, *2*(10), e585. doi: 10.1002/cpz1.585.

Weber, D. N., Fields, A. T., Patterson III, W. F., Barnett, B. K., Hollenbeck, C. M., & Portnoy, D. S. (2022). Novel epigenetic age estimation in wild-caught Gulf of Mexico reef fishes. *Canadian Journal of Fisheries and Aquatic Sciences*, *79*(1), 1-5. doi: https://doi.org/10.1139/cjfas-2021-0240.

Wegner, N. C., Lai, N. C., Bull, K. B., & Graham, J. B. (2012). Oxygen utilization and the branchial pressure gradient during ram ventilation of the shortfin mako, *Isurus oxyrinchus*: is lamnid shark–tuna convergence constrained by elasmobranch gill morphology?. *Journal of Experimental Biology*, *215*(1), 22-28. doi: https://doi.org/10.1242/jeb.060095.

Wegner, N. C., Sepulveda, C. A., Aalbers, S. A., & Graham, J. B. (2013). Structural adaptations for ram ventilation: gill fusions in scombrids and billfishes. *Journal of Morphology*, *274*(1), 108-120. doi: https://doi.org/10.1002/jmor.20082.

WILSON, C. A., & DEAN, J. M. (1983). The Potential Use of Sagittae for Estimating Age of Atlantic Swordfish, *Xiphias gladius*[1]. In *Proceedings of the International Workshop on Age Determination of Oceanic Pelagic Fishes: Tunas, Billfishes and Sharks, Southeast Fisheries Center, Miami Laboratory, National Marine Fisheries Service, NOAA, Miami, Florida, Feb. 15-18, 1982* (Vol. 8, p. 150). US Department of Commerce, National Oceanic and Atmospheric Administration, National Marine Fisheries Service, Scientific Publications Office.

Wootton, R. J., & Smith, C. (2014). *Reproductive biology of teleost fishes*. John Wiley & Sons.

Young J., Drake A., Brickhill M., Farley J., Carter T. (2003). Reproductive dynamics of broadbill swordfish, *Xiphias gladius*, in the domestic longline fishery off eastern Australia. *Marine and Freshwater Research*, 54: 315-332. doi: https://doi.org/10.1071/MF02011.

Zhang, Q., Vallerga, C. L., Walker, R. M., Lin, T., Henders, A. K., Montgomery, G. W., ... & Visscher, P. M. (2019). Improved precision of epigenetic clock estimates across tissues and its implication for biological ageing. *Genome medicine*, *11*, 1-11. doi: https://doi.org/10.1186/s13073-019-0667-1.

SITOGRAPHY

https://www.iccat.int/en/